Zootaxa 5397 (4): 451–485
https://www.mapress.com/zt/

Article

ISSN 1175-5326 (print edition)
ZOOTAXA
ISSN 1175-5334 (online edition)

https://doi.org/10.11646/zootaxa.5397.4.1
http://zoobank.org/urn:lsid:zoobank.org:pub:2F745EBA-05B4-4F85-A0EE-A56A73683B7A

Unexpected diversity and co-occurrence of phytotelmic frogs (*Guibemantis*) around Andasibe, one of the most intensively surveyed amphibian hotspots of Madagascar, and descriptions of three new species

HUGH GABRIEL[1], LAILA-DENISE ROTHE[1], JÖRN KÖHLER[2], SANDRATRA RAKOTOMANGA[3], DEVIN EDMONDS[4], PEDRO GALÁN[5], FRANK GLAW[6], RICHARD M. LEHTINEN[7], ANDOLALAO RAKOTOARISON[8,9] & MIGUEL VENCES[1*]

[1]*Zoologisches Institut, Technische Universität Braunschweig, Mendelssohnstr. 4, 38106 Braunschweig, Germany.*
hugh.tgabriel@gmail.com; https://orcid.org/0009-0002-0777-5709
l.rothe@tu-braunschweig.de; https://orcid.org/0009-0004-1595-0241
[2]*Hessisches Landesmuseum Darmstadt, Friedensplatz 1, 64283 Darmstadt, Germany.*
joern.koehler@hlmd.de; https://orcid.org/0000-0002-5250-2542
[3]*Mention Zoologie et Biodiversité Animale, Université d'Antananarivo, BP 906, Antananarivo, 101 Madagascar.*
sandratrapro@gmail.com; https://orcid.org/0009-0005-1825-9226
[4]*Illinois Natural History Survey, University of Illinois Urbana-Champaign, USA.*
dae2@illinois.edu; https://orcid.org/0000-0002-5633-7206
[5]*Universidad de A Coruña, Facultad de Ciencias, Campus de A Zapateira, s/n, (Grupo de Investigación en Biología Evolutiva, GIBE), E-15071 A Coruña, Spain.*
pedro.galan@udc.es; https://orcid.org/0000-0002-1681-3343
[6]*Zoologische Staatssammlung München (ZSM-SNSB), Münchhausenstr. 21, 81247 München, Germany.*
glaw@snsb.de; https://orcid.org/0000-0003-4072-8111
[7]*The College of Wooster, Department of Biology, 931 College Mall, Wooster, Ohio, 44691 USA.*
rlehtinen@wooster.edu; https://orcid.org/0000-0002-4784-4660
[8]*Mention Agriculture, Universite de l'Itasy, Faliarivo Ambohidanerana, 118 Soavinandriana Itasy, Madagascar.*
[9]*School for International Training, VN 41A Bis Ankazolava Ambohitsoa, Antananarivo, 101 Madagascar.*
andomailaka@gmail.com; https://orcid.org/0000-0003-2620-440X
[*]*Corresponding author: m.vences@tu-braunschweig.de; https://orcid.org/0000-0003-0747-0817*

Abstract

The area around the Malagasy village of Andasibe, which includes Analamazaotra-Mantadia National Park as well as other protected areas, is characterized by very species-rich and well-studied communities of animals and plants, but new species are still regularly discovered. Three species of phytotelmic frogs of the subgenus *Pandanusicola* in the genus *Guibemantis* are known from this area, *G. flavobrunneus, G. liber*, and *G. pulcher*. Further *Pandanusicola* frogs from this area have been provisionally assigned to *G. bicalcaratus* or *G. albolineatus,* pending detailed taxonomic review. During preliminary exploration of the ecology of these specialized frogs that live and reproduce in the leaf axils of *Pandanus* screw pines, we noticed the syntopic presence of two differently colored and differently sized *Pandanusicola* in Andasibe that could not be unambiguously assigned to any known species. A genetic screening revealed that these correspond to yet two further species in the area. Based on our data, seven species of *Pandanusicola* occur in Andasibe and nearby forests: (1) *G. liber,* the only non-phytotelmic species of the subgenus in the region; (2) *G. flavobrunneus* which is the largest species and characterized by a diagnostic yellowish brown dorsal pattern; (3) *G. pulcher,* characterized by translucent-green color with purplish brown spotting not observed in any other species in the area; (4) *G. methueni*, a brownish species usually lacking contrasted dorsolateral bands that differs from the other species in the area by emitting a characteristic trill-like advertisement call series (rather than clicks or chirps) and according to our data is widespread along Madagascar's east coast; as well as three new species: (5) *G. ambakoana* **sp. nov.**, a brownish species, typically with contrasted incomplete light dorsolateral bands and with single click-like advertisement calls; (6) *G. vakoa* **sp. nov.**, a species that is equally brownish but lacks contrasted light dorsolateral bands and that has single click-like advertisement calls of very short duration; and (7) *G. rianasoa* **sp. nov.**, a species that is smaller sized and has less distinct femoral glands than all the others, and emits a short series of soft chirp-like advertisement calls. All these species are genetically highly distinct, with >5% uncorrected pairwise distances in the mitochondrial 16S rRNA gene, and lack of haplotype sharing in two nuclear-encoded genes. The co-occurrence of seven *Pandanusicola* frogs in a relatively small geographic area is unprecedented in Madagascar and calls for in-depth studies of a possible differentiation in habitat use and life history.

Accepted by D.C. Blackburn: 21 Nov. 2023; published: 8 Jan. 2024

Key words: Amphibia, Anura, Mantellidae, *Pandanusicola*, *Guibemantis rianasoa* **sp. nov.**, *Guibemantis ambakoana* **sp. nov.**, *Guibemantis vakoa* **sp. nov.**, *Pandanus*, bioacoustics, phytotelmic breeding, microendemism, sympatry, phylogeny, systematics, taxonomy

Introduction

The island of Madagascar is exceptionally biodiverse and characterized by a high degree of endemism due to its longstanding isolation situated about 400 km off the East coast of the African continent (e.g., Crottini *et al.* 2012). Its astonishing species richness likely originated from a combination of diversification mechanisms such as the mountain refuge, riverine barrier and watershed refuge processes (Brown *et al.* 2014, 2016). Contributing to its diversity is an impressive number of 412 species of frogs (AmphibiaWeb 2023), of which 408 (all except two introduced species) are endemic to the island. Unfortunately, destruction of natural vegetation in Madagascar is ongoing, with 44% of the island's forests lost between 1953 and 2014 (Vieilledent *et al*. 2018), and consequently, much of Madagascar's biodiversity is threatened.

The area around the village of Andasibe (previously named Périnet) on the eastern slopes of Central Madagascar is renowned for its extreme species diversity (Lees 1994; Colwell & Lees 2000), including at least 94 species of amphibians (Vieites *et al.* 2009). This area is one of the best studied in Madagascar, comprising the Analamazaotra-Mantadia National Park and various other protected areas. Still, the incredible species richness of the primary and secondary humid forests in the region continues to yield new discoveries in biodiversity (Goodman 2010), including amphibians (e.g., Glaw *et al.* 2021; Miralles *et al.* 2023).

Among Malagasy frogs of the families Mantellidae and Microhylidae, several species are phytotelmic specialists, dwelling and reproducing in *Pandanus* plants and with parent-attended young observed in some species (Lehtinen 2003; see also an updated list of phytotelm-breeding frogs at https://sites.google.com/site/phytotelmbreedingfrogsworld/). Commonly known as "screw pines", *Pandanus* trees or shrubs are characterized by long, pointed leaves with lateral spines that radiate outwards from a central point on the stem. Facilitated by the unique shape of these leaves, many *Pandanus* species accumulate water in their leaf axils (Guillaumet 1973). Madagascar is home to 79 endemic species of *Pandanus* (Callmander *et al.* 2022), and many water-dependent animal species live in those *Pandanus* with phytotelmic leaf axils. Some frog species are considered "*Pandanus* obligates", spending their entire life cycle within the habitat provided by one tree (Lehtinen 2002).

Within Mantellidae, one clade of the genus *Guibemantis* is classified as the subgenus *Pandanusicola* (Glaw & Vences 1994, 2006). The majority of species in this subgenus are *Pandanus* obligates (Glaw & Vences 2007), notwithstanding that five *Pandanusicola* species, *G. fotsitenda*, *G. liber*, *G. razandry*, *G. razoky*, and *G. tasifotsy*, only use *Pandanus* leaf axils to rest and hide during the day. After an initial assessment by Lehtinen *et al.* (2007), it became clear that the genus contained a large amount of undiscovered diversity. Subsequent revisions (Lehtinen *et al.* 2012, 2018, Vences *et al.* 2013, 2023; Bletz *et al.* 2018; Koppetsch *et al.* 2023) have brought the total number of species in the subgenus to 18. Studies of activity (Heinermann *et al.* 2015), reproductive habits (Lehtinen 2003), larval ecology (Lehtinen 2004), interspecific competition (Lehtinen 2005), longevity (Lehtinen 2009), and the herpetological species diversity hosted by *Pandanus* (Lehtinen 2002) have helped to paint a fuller picture of *Pandanus* obligate frogs on the whole. However, a substantial number of unconfirmed and confirmed candidate species in *Pandanusicola* identified by Lehtinen *et al.* (2007) and Vieites *et al.* (2009) have still not been addressed taxonomically.

Pandanus trees are common in the Andasibe area, and *Pandanusicola* frogs are long known from this part of Madagascar. Blommers-Schlösser (1975) first observed the unique mating behavior of mantellines, without amplexus, in *G. liber* at Andasibe. She later also recorded *G. pulcher* from Andasibe, and described a new species, *G. flavobrunneus*, from this site (Blommers-Schlösser 1979). Besides these relatively distinct species, subsequent work reported additional *Pandanusicola* from Andasibe that were tentatively assigned to *G. bicalcaratus* or *G. albolineatus* (e.g., Glaw & Vences 1994) and later considered as candidate species (e.g., Vieites *et al.* 2009). However, an in-depth revision of these frogs in the Andasibe region is so far missing, and almost nothing is known about their biology, given that the majority of the natural and life history studies available to date (e.g., Lehtinen 2002, 2003, 2005, 2009) refer to *Pandanusicola* species from the South East of Madagascar.

During preliminary exploration of the ecology of these frogs, we noticed the syntopic presence of two differently colored and differently sized *Pandanusicola* frogs in Andasibe that did not fully match any of the nominal species

in morphology and coloration. This motivated us to undertake focused collections and a comprehensive genetic screening of all *Guibemantis* samples available to us. As a result, the existence of four additional species of *Guibemantis* in the Andasibe area was revealed, of which one represented a range extension of an existing species (*G. methueni*) and three turned out to be new to science. Here, we report these observations and formally name and describe the three new species.

Material and Methods

Sampling

A survey of *Pandanus* obligate frogs was conducted by HG at various sites near Andasibe from 19 April to 1 May 2022, including Analamazaotra Forest Station (= "Mitsinjo Park"), and Mantadia National Park. Data were collected on a tree-by-tree basis, with 253 individual *Pandanus* trees examined, snout-vent length recorded for frogs captured, and photos of dorsal and ventral views taken from selected individuals. Given the observation of various syntopically occurring and morphologically distinct unknown *Guibemantis* species, additional collecting work was carried out during 14–15 June 2022 by AR and 17–18 November 2022 by MV, SR, and PG.

In addition to the fieldwork conducted in 2022, voucher specimens and tissue samples used for this study were collected during other field surveys between 2000–2021. Frogs were caught by specifically searching in *Pandanus* plants, mostly during the day. Voucher specimens were anesthetized by immersion in MS222 solution and subsequently euthanized with an overdose of the same substance. We then immediately took a tissue sample of each specimen for molecular analysis, typically a part of the thigh muscle, and stored it in a 1.5 ml vial with pure ethanol. Subsequently, the specimens were fixed in 95% ethanol and preserved in 70% ethanol, and deposited in the following collections: Université d'Antananarivo, Département de Biologie Animale (UADBA), Zoological Museum Amsterdam (ZMA; collections now in Naturalis, Leiden), and Zoologische Staatssammlung München (ZSM). We use DRV, FGZC, FGMV, ZCMV, PSH and THC to refer to the field numbers of D. R. Vieites, F. Glaw and M. Vences, P.-S. Gehring, and T. R. Fulgence, respectively. A full list of all field numbers and museum catalogue numbers, as well as sequences and sequence accession numbers, is available as Excel and tab-delimited table from the Zenodo repository under DOI 10.5281/zenodo.10028230. The majority of the vouchers deposited in UADBA have not yet been catalogued in that collection, and they are therefore referenced by their respective field numbers.

Morphology

The following measurements were taken by MV from preserved voucher specimens using a manual caliper at an accuracy of 0.1 millimeter: snout–vent length (SVL); maximum head width (HW); head length from tip of snout to posterior edge of snout opening (HL); horizontal tympanum diameter (TD); horizontal eye diameter (ED); distance between anterior edge of eye and nostril (END); distance between nostril and tip of snout (NSD); distance between both nostrils (NND); forelimb length, from limb insertion to tip of longest finger (FORL); hand length, from base of the palm to the tip of the longest finger (HAL); hind limb length, from the cloaca to the tip of the longest toe (HIL); foot length (FOL); foot length including tarsus (FOTL); and tibia length (TIBL), FGL (maximum length of femoral gland along axis of shank), FGW (maximum femoral gland width). Geographical regions within Madagascar are named according to Boumans *et al.* (2007). Femoral glands are classified according to Glaw *et al.* (2000) and Vences *et al.* (2007).

Bioacoustics

We recorded vocalizations in the field over the years using different types of tape recorders (Tensai RCR-3222, Sony WM-D6C) with external microphones (Sennheiser Me-80, Vivanco EM 238), and with digital recorders with built-in microphones (Edirol R-09, Tascam DR 05x). Recordings were sampled or re-sampled at 22.05 kHz and 32-bit resolution and analyzed using the software Cool Edit Pro 2.0. We obtained frequency information through

Fast Fourier Transformation (FFT; width 1024 points) at Hanning window function. Spectrograms were produced at Blackman window function with 256 bands resolution. Sensitive filtering was used to remove background sounds, applied only to frequencies outside the prevalent bandwidths of calls. Temporal measurements are summarized as range with mean ± standard deviation in parentheses. Terminology and methods in call analyses and descriptions follow the recommendations and call-centered terminological scheme of Köhler *et al.* (2017), as also applied by Koppetsch *et al.* (2023) for calls of the *Guibemantis liber* species complex. Call recordings were deposited at the Zenodo repository (DOI: 10.5281/zenodo.10028230).

Molecular genetics

For molecular analyses, we extracted DNA from ethanol-preserved tissue samples using a standard salt extraction protocol (Bruford *et al.* 1992). To obtain an overview of the puzzling genetic variation in *Guibemantis*, we used a fragment of the mitochondrial 16S rRNA gene (16S) used previously for molecular taxonomy of Malagasy frogs (e.g., Vieites *et al.* 2009), spanning about half of the gene at its 3' terminal portion. From new samples, the 16S fragment was amplified with primers 16SAL (5'–CGCCTGTTTATCAAAAACAT–3') and 16SBH-new: (5'–CCTGGATTACTCCGGTCTGA–3'), modified from Palumbi *et al.* (1991), with the following cycling protocol: 94°C (90s), [94°C (45s), 55°C(45s), 72°C (90s) x 33], 72°C (300s). The new sequences were complemented by all reliably identified sequences of this gene fragment for *Guibemantis* that could be retrieved from GenBank.

In addition to 16S, we sequenced two fragments of nuclear-encoded protein-coding genes from the focal lineages and morphologically similar or phylogenetically related species. This included a fragment of the recombination activating gene 1 (RAG-1), using primers Gephlut-RAG1-F1 (5'–ATGGAGAGCCAACCCCTATC–3') and Gephlut-RAG1-R1 (5'–KCCAGACTCGTTTCCTTCRC–3'), and the sequencing primer RAG1-Manti-Seq1 (5'–GCAAAGCCVTTTATTGAAACC–3'), with cycling protocol: 94°C (120s), [94°C (20s), 54°C (50s), 72°C (180s) x 39], 72°C (600s) (Vences *et al.* 2021a); and a fragment of sacsin (SACS), amplified with a nested PCR approach following Shen *et al.* (2012) using external primers SACSF2 (5'–AAYATHACNAAYGCNTGYTAYAA–3') and SACSR2 (5'–GCRAARTGNCCRTTNACRTGRAA–3') and internal primers SACSNF2 (5'–TGYTAYAAYGAYTGYCCNTGGAT–3') and SACSNR2 (5'–CKGTGRGGYTTYTTRTARTTRTG–3') and with cycling protocol for both PCRs: 94°C(240s), [94°C (45s), 45°C (40s), 72°C (120s)] x 45, 72°C (600s).

PCR products were purified with Exonuclease I and Shrimp Alkaline Phosphatase digestion and sent for sequencing on automated DNA sequencers to LGC Genomics (Berlin). Chromatograms were checked and corrected for obvious errors with CodonCode Aligner 3.7.1 (Codon Code Corporation, Dedham, MA, USA). All newly obtained sequences were submitted to GenBank and are available under the following accession numbers: OR689491–OR689554 and OR689922–OR690024.

16S sequences were aligned with MAFFT v. 7.222 (Katoh & Standley 2013) as implemented in iTaxoTools (Vences *et al.* 2022), and a phylogeny inferred with RAxML (Stamatakis 2014) using raxmlGUI v. 2.0 (Edler *et al.* 2021) under the Maximum Likelihood (ML) optimality criterion, after selecting the most appropriate substitution model based on the Bayesian Information Criterion in MEGA7. Node support was assessed with 1000 bootstrap replicates using the "thorough bootstrap" option.

For lineage delimitation, molecular diagnosis, and calculation of genetic distances, we used a trimmed alignment, which was prepared using the following criteria: removal of sequences with an excessive number of missing data at the beginning and end, and trimming of alignment positions at the beginning and end, but maintaining at least one sequence of each nominal taxon or major lineage a priori recognizable in the ML tree. After MAFFT realignment, this alignment contained 470 nucleotide positions, with a maximum of 12 missing nucleotides per sequence (except for the single sequence of *G.* sp. Ca19 which was maintained in the data set despite having 24 missing nucleotides). We then submitted this alignment to an initial lineage delimitation ASAP (Puillandre *et al.* 2021), determination of diagnostic nucleotide positions (given relative to the full 16S rRNA gene sequence of *Mantella madagascariensis*; accession number AB212225) using MolD (Fedosov *et al.* 2022), and calculation of uncorrected pairwise distances using TaxI2 (Vences *et al.* 2021b). The alignment file is available from the Zenodo repository under DOI 10.5281/zenodo.10028230. The MolD analysis provides a robust diagnostic nucleotide combination that represents a small set of maximally informative molecular character states defining a species in comparison with all included congeners, and is here presented mainly as a means to formally fulfill the requirements of the Code to present diagnostic characters (i.e., not just genetic distances) in words.

We used a network approach for graphically representing the relationship among alleles (haplotypes) of the RAG-1 and SACS fragments. Sequences of these genes were aligned using the Clustal algorithm implemented in MEGA7 (Kumar *et al.* 2016), alleles (haplotypes) inferred with the PHASE algorithm (Stephens *et al.* 2001) implemented in the DnaSP software (Version 5.10.3; Librado & Rozas 2009), an ML tree inferred under the Jukes-Cantor substitution model in MEGA7 (choosing this simple model to avoid overparametrization). This tree together with the respective alignment was then used as input for Haploviewer (written by G.B. Ewing; http://www.cibiv.at/~greg/haploviewer), a software that implements the methodological approach of Salzburger *et al.* (2011).

Rationale for species delimitation

To delimit species, we follow a general lineage concept (de Queiroz 1998, 2007) in combination with a relaxed biological species criterion, i.e., demanding reproductive isolation indicated by restricted gene flow among lineages (e.g., Speybroeck *et al.* 2020). As lines of evidence supporting this species criterion, we primarily rely on (i) sympatric or geographically adjacent occurrence of two lineages without free admixture in mitochondrial and unlinked nuclear loci (i.e., genealogical concordance; Avise & Ball 1990) which strongly suggests the absence of hybridization or very narrow hybrid zones and thus distinct species (e.g., Dufresnes *et al.* 2021; Pyron *et al.* 2023); (ii) differences in advertisement calls, particularly in general call structure and mostly static characters such as note duration (Köhler *et al.* 2017). We furthermore rely on phylogenetic position, considering lineages placed distant from each other in the multigene *Guibemantis* tree of Koppetsch *et al.* (2023) and thus not constituting sister lineages, to most likely represent distinct species. The rationale outlined above thus implies that the delimitation and formal naming of species does not necessitate morphological divergence, which aligns with evidence for the existence of truly cryptic species in other taxa (Jörger & Schrödl 2013; Delić *et al.* 2017; Fišer *et al.* 2018; Glaw *et al.* 2021).

Results

Molecular differentiation and evolutionary relationships of *Guibemantis*

The ML tree based on the 16S alignment of 545 bp for 368 *Guibemantis* individuals confirmed the existence of a large number of mitochondrial lineages within *Guibemantis* (Fig. 1). The species partition with the best ASAP score of 4.0 supported as many as 60 species-level subsets within the genus *Guibemantis*, while other suggested species partitions contained 35–61 subsets. A graph with the ten selected species partitions is available at DOI 10.5281/zenodo.10028230. All nominal species as well as numerous other candidate species were supported in one or several of these partitions, and many were subdivided into additional smaller units. To avoid taxonomic over-splitting, we followed the recommendations of Puillandre *et al.* (2021) and modified the information from ASAP 16S-based species partitions conservatively, in part based on comprehensive integrative evidence – e.g., in the *G. liber* complex where the 16S tree data suggest *G. razoky* being phylogenetically nested within *G. liber,* and *G. liber* and *G. razoky* consisting of various lineages, which is largely contradicted by phylogenomic data (Vences *et al.* 2023). We thus attempted to conservatively match ASAP lineages as closely as possible to nominal species and to numbered candidate species (*Guibemantis* sp. Ca1 to Ca21) according to the scheme established by Vieites *et al.* (2009) and refined by Perl *et al.* (2014). All the focal lineages in the wider Andasibe region were supported by ASAP, confirming their status as distinct species-level subsets, with some even exhibiting further subdivisions.

Samples from Andasibe and nearby sites (Fig. 2) belonged to seven of these lineages: the two well-defined species (i) *G. pulcher* and (ii) *G. flavobrunneus*; (iii) *G. methueni,* a species quite common at coastal localities in the Northern Central East and, according to the mitochondrial data, also occurring at Besariaka south of Moramanga, and Andasibe; (iv) a lineage corresponding to relatively small-sized and greenish colored specimens from Andasibe, which is here interpreted as including the previously defined *G.* sp. Ca14 from Fierenana, and thus referred to under this name; (v) a lineage of brownish-colored frogs that genetically matches the previously defined *G.* sp. Ca3 or (= *G.* sp. aff. *albolineatus*) from Andasibe; (vi) a further brownish-colored species not found at Andasibe but occurring nearby at Besariaka (near Moramanga), Fierenana, Sahafina, and Betampona, which we here assign to the candidate species *G.* sp. Ca8 (= *G.* sp. aff. *bicalcaratus* "Moramanga"), but noting that in Vieites *et al.* (2009) a wrong voucher

number (ZCMV 466) was given for this lineage; and (vii) a further mitochondrial lineage of brown-colored frogs from Andasibe which had not been detected before, and which we name *G.* sp. Ca22. In addition, we here coin the candidate species names *G.* sp. Ca23 for a genetically highly divergent unconfirmed candidate species (UCS) from Nosy Boraha; *G.* sp. Ca24 for a morphologically and genetically confirmed candidate species (CCS) from Manombo; *G.* sp. Ca25 for a UCS from the Marojejy Massif; and *G.* sp. Ca26 for a UCS from Betampona and south of Maroantsetra with genetic affinities to *G. punctatus*.

It needs to be emphasized that the main goal of the 16S tree is to illustrate mitochondrial variation within *Guibemantis* and to cluster individuals into main lineages, but not to reliably reconstruct deep phylogenetic relationships within the genus for which longer sequences are necessary (Chan *et al.* 2022). A more reliable multigene tree of *Guibemantis* is included in Koppetsch *et al.* (2023). However, for the focal lineages, the current tree (Fig. 1) provides evidence that the co-occurring lineages are not each other's closest relatives. For instance, *G.* sp. Ca11, Ca22 and Ca24 are placed together in a clade, while *G. pulcher* and G. *flavobrunneus* are placed together in another clade, apparently unrelated to the other species occurring at Andasibe.

Pairwise uncorrected distances between and within all species and candidate species of *Guibemantis* are summarized in a table available at DOI 10.5281/zenodo.10028230. Distances between nominal species were in all cases >5%, except for those among the well-established species *G. flavobrunneus, G. pulcher*, and *G. pulcherrimus* that differed by 3.5–4.8%, and *G. kathrinae* and *G. tornieri* that differed by 2.4–4.1%. Divergences of candidate species to nominal species also were >5% (except for 4.8% between *G. bicalcaratus* and *G.* sp. Ca24), as were pairwise distances between candidate species (except for Ca16 vs. Ca24, 3.2%; Ca3 vs. Ca23, 3.9–4.6%; Ca8 vs. Ca23, 3.1–3.7%; Ca22 vs. Ca24, 4.1%).

Haplotype networks of the two nuclear-encoded gene fragments (RAG-1: 574 bp for 62 samples; SACS: 878 bp for 47 samples; Fig. 3) found extensive haplotype sharing among some of the mitochondrial lineages but distinct phylogroups without haplotype sharing for others. With respect to the focal lineages, we found that *G.* sp. Ca14 had distinct haplogroups in both nuclear-encoded genes, without any haplotype sharing with other lineages and differing from other haplotypes by a minimum of 3 (SACS) and 6 (RAG-1) mutational steps. On the other hand, frogs that were placed in the mitochondrial tree in the *G.* sp. Ca3 and Ca22 lineages, respectively, showed widespread haplotype sharing with each other both in RAG-1 and SACS; the phylogroup containing samples of these two mitochondrial lineages also contained *G. wattersoni* in RAG-1 but not in SACS (for which no *G. wattersoni* was sequenced). *G. methueni*, represented in the haplotype networks by numerous samples from different sites, did not share haplotypes with any other lineage in SACS, but shared RAG-1 haplotypes with *G. bicalcaratus* (two haplotypes), *G.* sp. Ca8 (one haplotype), and *G.* sp. Ca26 (one haplotype).

Bioacoustics

As *Pandanusicola* frogs usually call from within the spiny *Pandanus* plants, it is inherently difficult to observe a calling individual (i.e., seeing the inflation of its vocal sac during sound emission), and to subsequently catch the calling male in order to allocate the call recording to a genotyped voucher specimen. Nevertheless, by combining published data (Blommers-Schlösser 1979; Lehtinen *et al.* 2011; Vences *et al.* 2006, 2011) with new data, recordings in sufficient quality for comparisons were available from three nominal species (*G. annulatus, G. methueni*, *G. pulcher*), as well as three candidate species *G.* sp. Ca3, Ca8, Ca14) (Fig. 4). Despite an overall similarity, several obvious bioacoustic differences are apparent: *G. methueni* differs from all other species by emitting a short, trill-like series of calls (Fig. 4D), which we detected in specimens from Ambila-Lemaitso (Blommers-Schlösser 1979), Ankanin'ny Nofy, and Andasibe. *Guibemantis pulcher* emits single chirp-like notes of pulsatile character (Fig. 4F) in rather irregular succession (Vences *et al.* 2011), similar to *G. annulatus*, where the calls are however, less pulsatile (see Lehtinen *et al.* 2011 for details) and thus somewhat intermediate between clicks and chirps to the human ear. *Guibemantis* sp. Ca14 emits a short series of 2–3 pulsatile calls of relatively low intensity (Fig. 4A), with the first call of a call series being lower in intensity and dominant frequency compared to subsequent calls of the same series. *Guibemantis* sp. Ca3 (Fig. 4B) and *G.* sp. Ca8 (Fig. 4C) emit rather loud click-like calls separated by long intervals of about 620–2520 ms, with calls of *G.* sp. Ca8 being shorter in duration (without overlap) compared to those of *G.* sp. Ca3 (3–14 vs. 20–93 ms). See Appendix 1, Lehtinen *et al.* (2011), and Vences *et al.* (2011) for details. Overall, the observed call differences between several of the nominal species and candidate lineages are in support of genetic results and thus substantiate the species status of the respective clades.

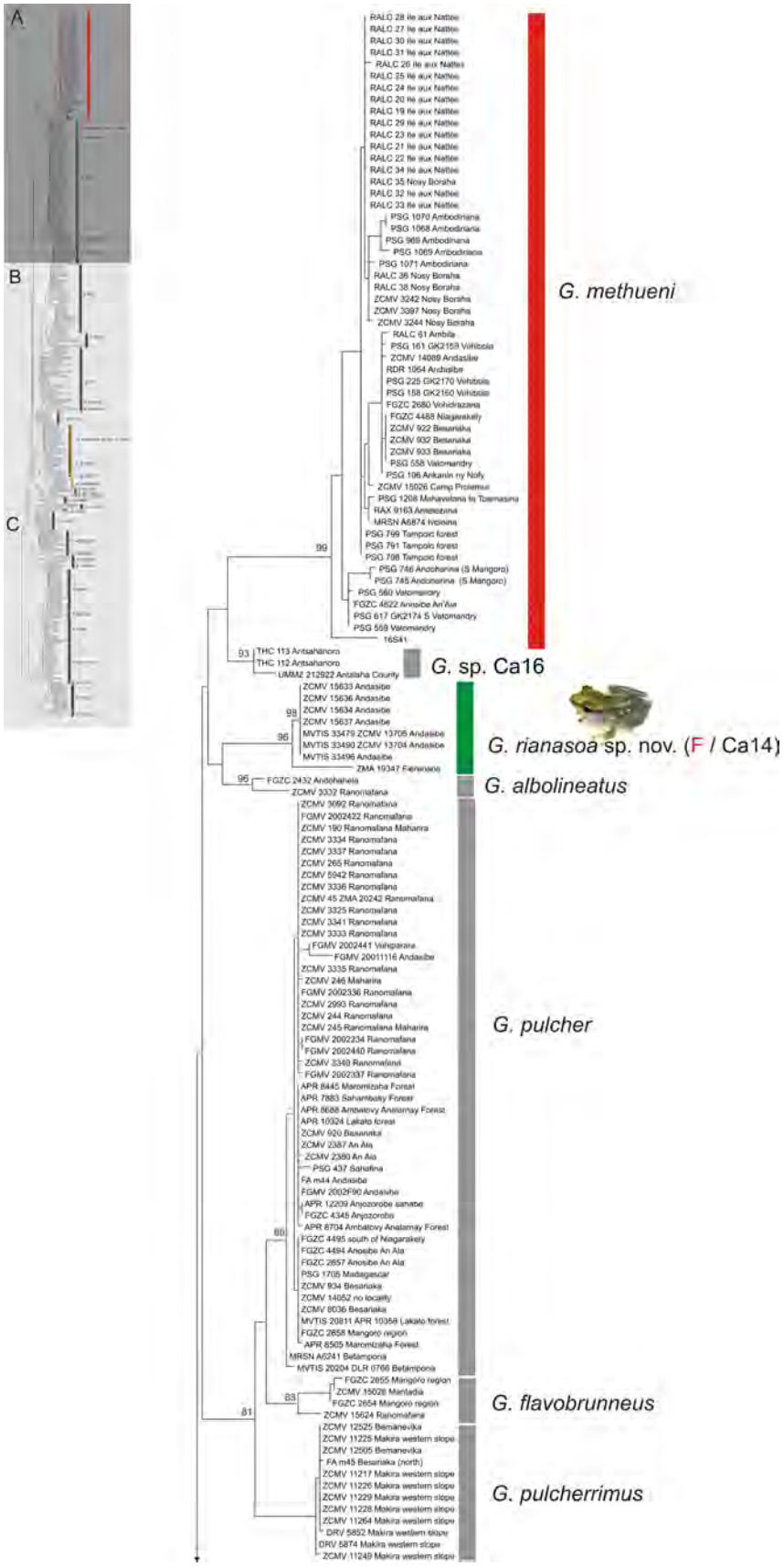

FIGURE 1. Maximum Likelihood tree based on a DNA sequences of a fragment of the mitochondrial 16S rRNA gene (alignment length 545 bp) for 368 specimens of all species and candidate species of *Guibemantis*. See Koppetsch *et al.* (2023) for a discussion of the mitochondrial non-monophyly of species in the *G. liber* complex (*G. fotsitenda*, *G. liber*, *G. razandry*, *G. razoky*).

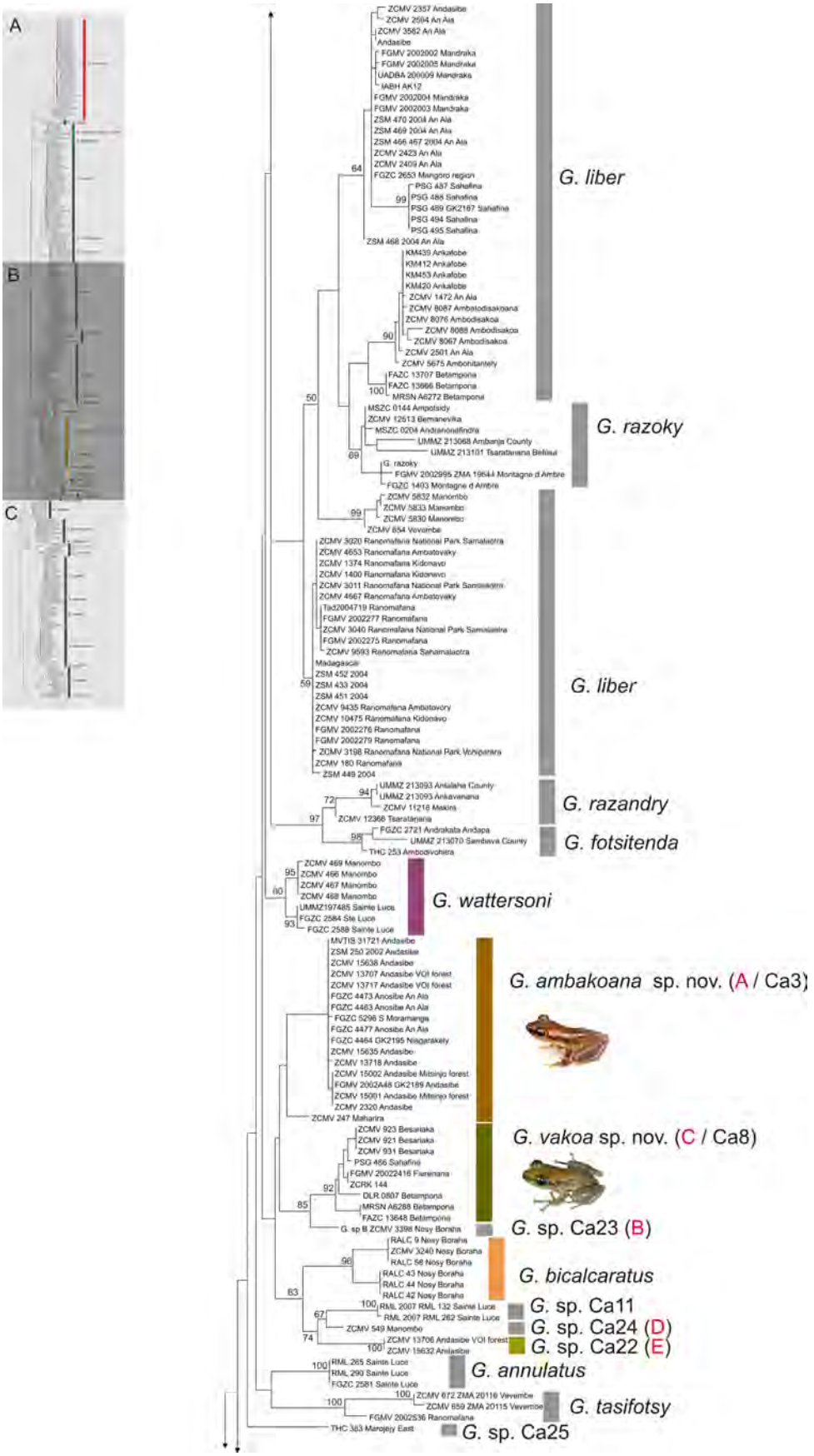

FIGURE 1. (Continued)

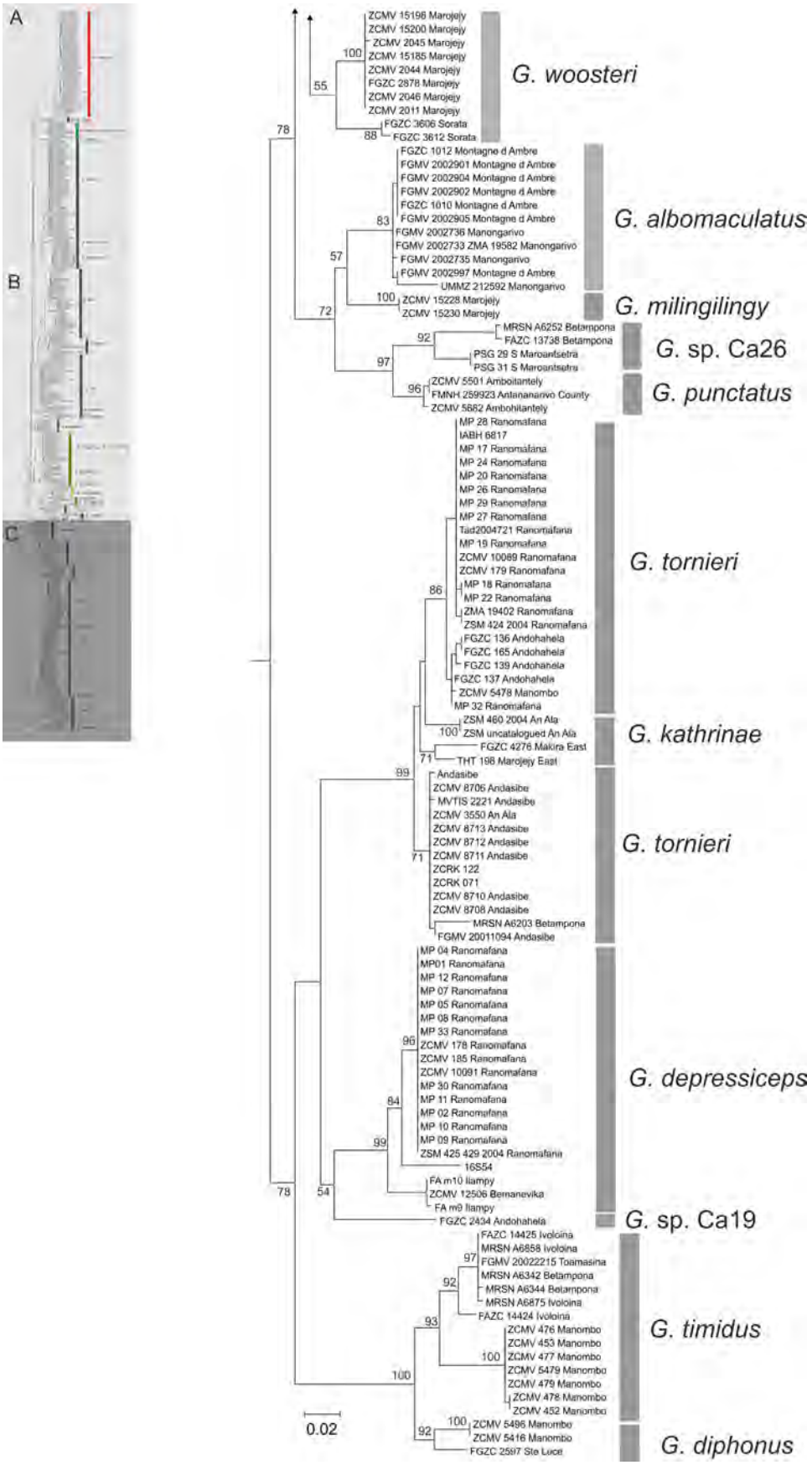

FIGURE 1. (Continued)

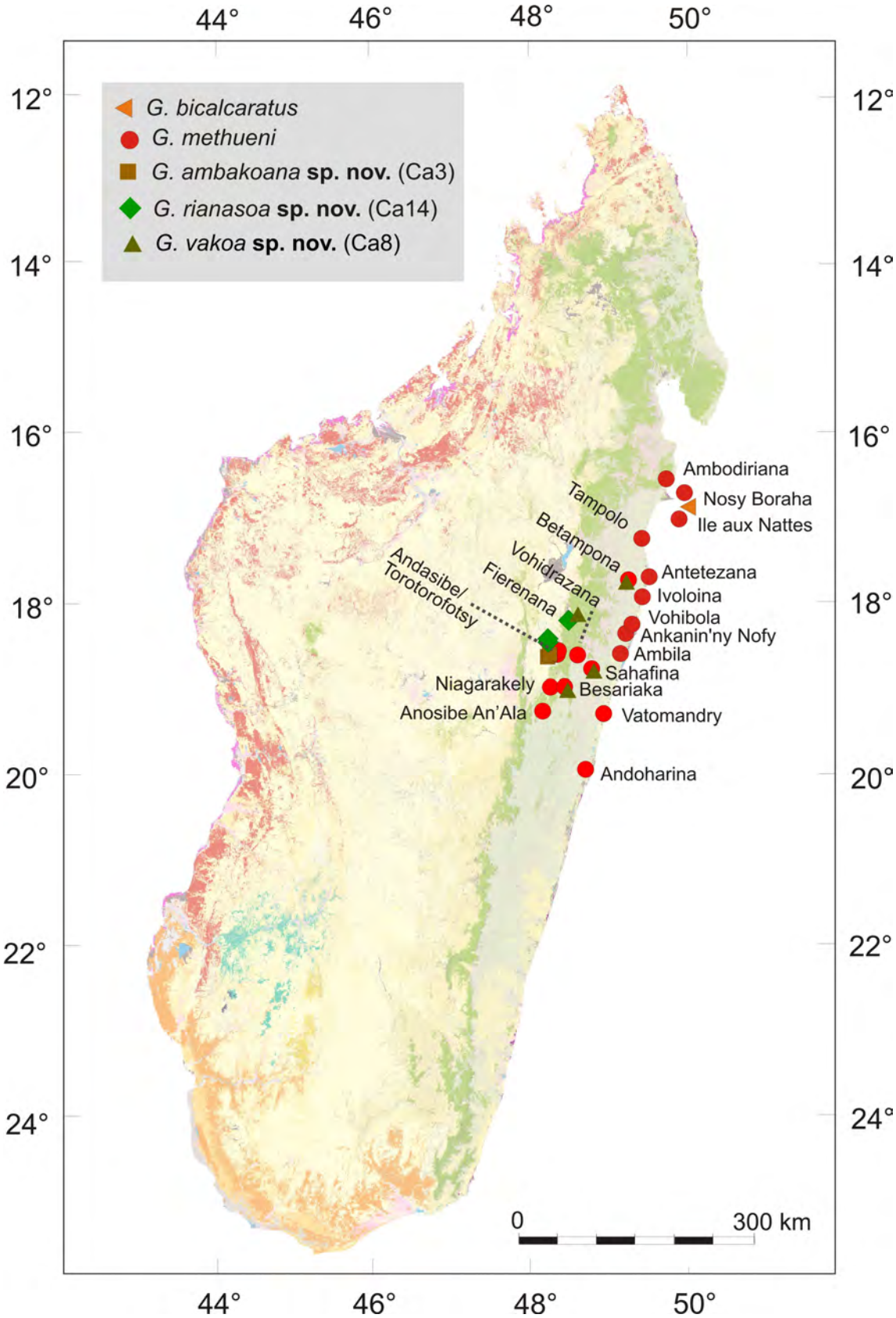

FIGURE 2. Map of Madagascar showing genetically verified locality records of the target species of *Guibemantis* studied herein (colors as in Fig. 1). The base map shows vegetation across Madagascar from the Madagascar Vegetation Mapping Project (Moat & Smith 2007; formerly available at www.vegmad.org). Vegetation is colored as follows: green, humid forest (rainforest); red, western dry deciduous forest; bluish, western subhumid forest; orange, south western dry spiny forest-thicket; yellow, tapia forest.

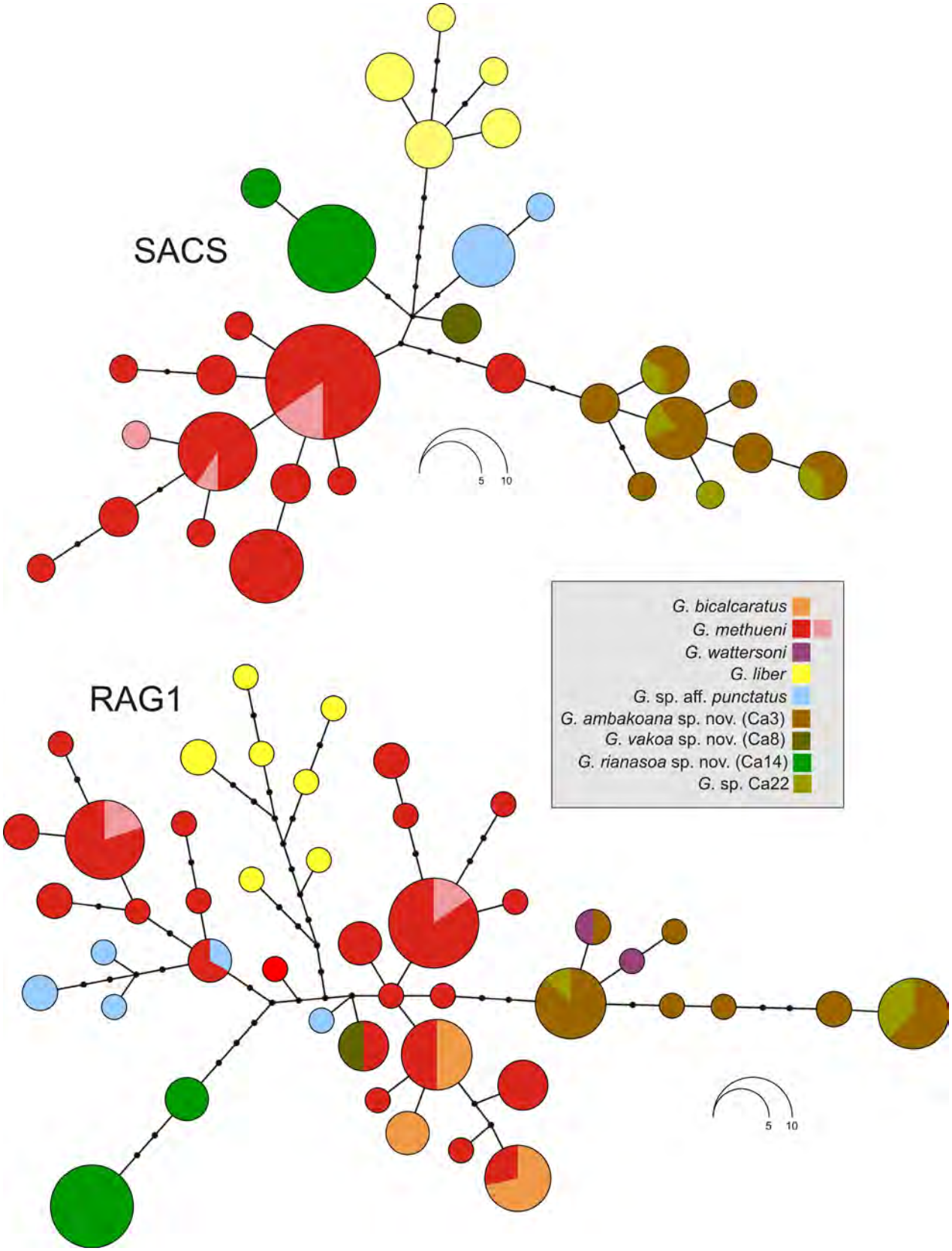

FIGURE 3. Haplotype networks of phased sequences of fragments of the nuclear-encoded genes for SACS (47 samples for 878 bp) and RAG-1 (62 samples for 574 bp) from the target species plus selected *Guibemantis* outgroup species. Haplotypes are colored according to their assignment to lineages in the mitochondrial tree (Fig. 1). Light red (pink) color denotes specimens for which no mitochondrial sequences were available but which, based on their collecting locality, very likely belong to *G. methueni*.

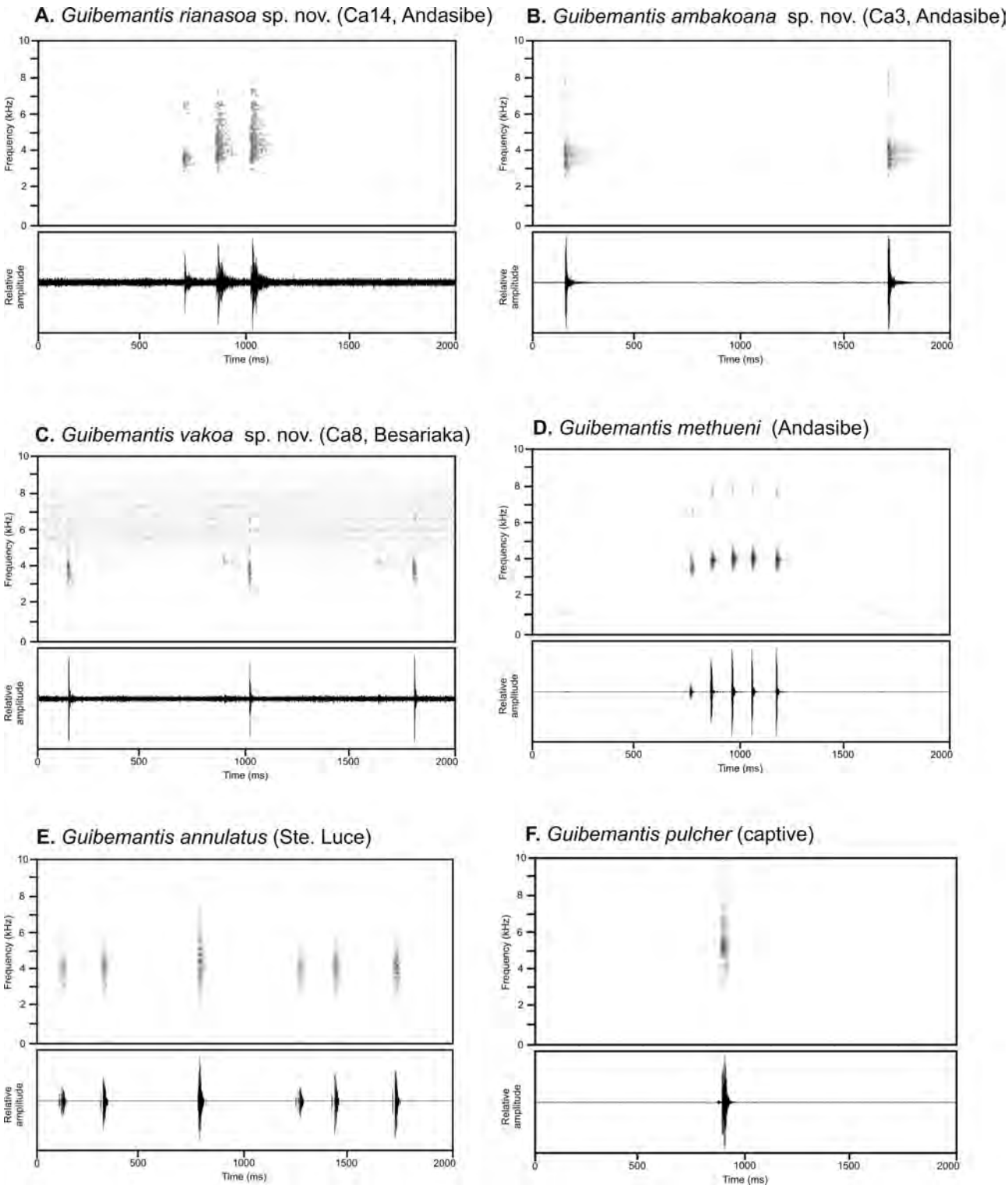

FIGURE 4. Audiospectrograms and oscillograms of advertisement calls of six species of *Guibemantis* of the subgenus *Pandanusicola*. **A**, call series (containing 3 calls) of *Guibemantis rianasoa* **sp. nov.**, recorded on 19 November 2022 at Andasibe. Recording high-pass filtered at 2000 Hz. **B**, two calls of *Guibemantis ambakoana* **sp. nov.**, recorded on 19 November 2022 at Andasibe. Recording high-pass filtered at 1500 Hz. **C**, three calls of *Guibemantis vakoa* **sp. nov.** recorded on 15 February 2004 at Besariaka. Recording band-pass filtered at 1500–9200 Hz. **D**, call series (containing 5 calls) of *Guibemantis methueni* recorded on 8 November 2011 at Andasibe. Recording high-pass filtered at 1000 Hz. **E–F, c**alls of *G. annulatus* (from Lehtinen *et al.* 2011) and *G. pulcher* (from Vences *et al.* 2011).

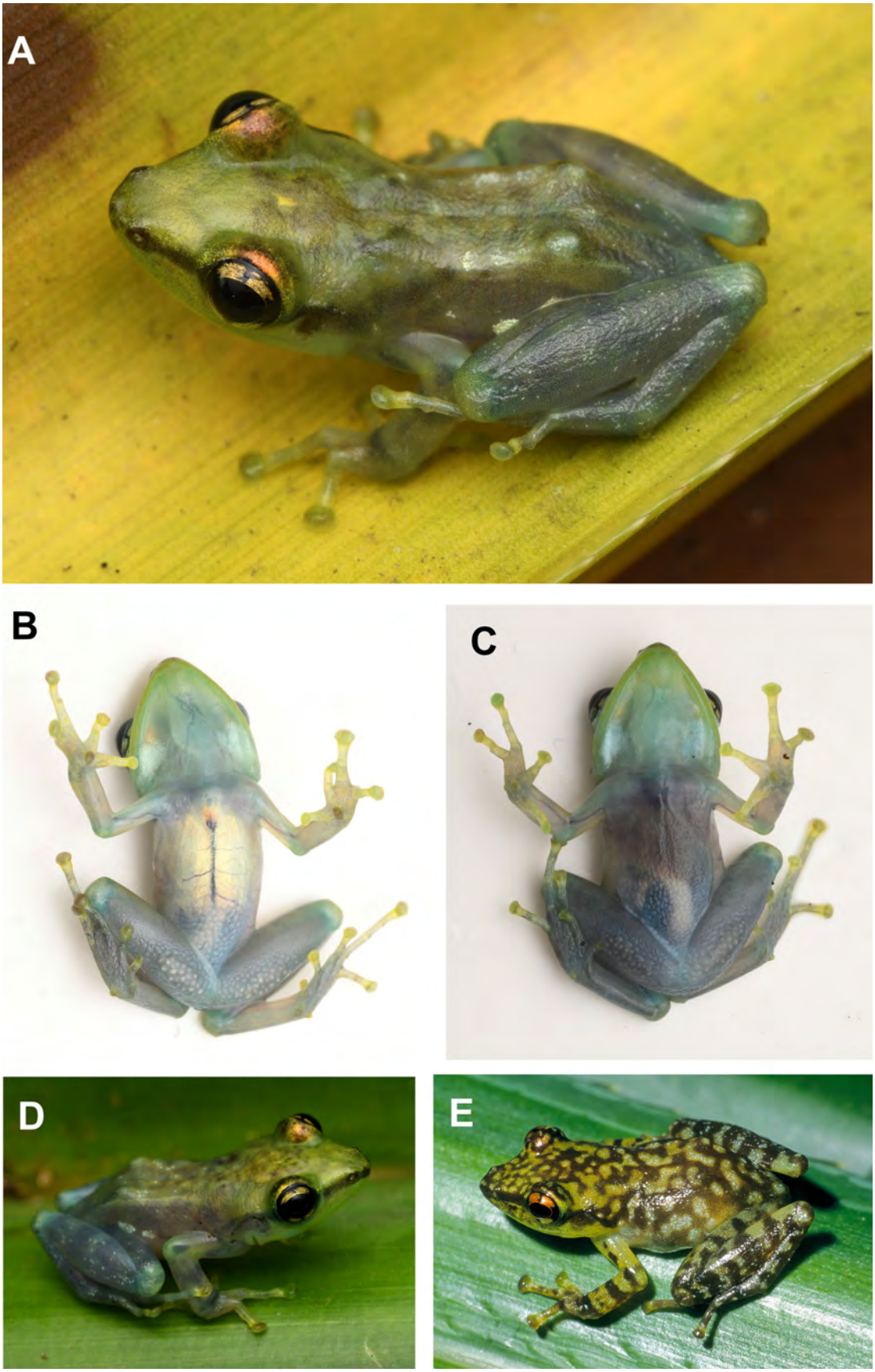

FIGURE 5. *Guibemantis rianasoa* **sp. nov.** (sp. F / Ca14) in life. **A–B.** Male holotype ZSM ZSM 149/2022 (ZCMV 13705) from Andasibe VOI forest in dorsolateral and ventral view; **C–D.** Male paratype ZSM ZSM 148/2022 (ZCMV 13704) in ventral and dorsolateral view. **E.** Specimen from Fierenana (ZMA 19347; FGMV 2002.2418) in dorsolateral view.

Morphological differentiation

During the field survey in April 2022, *Pandanusicola* specimens were morphologically assigned to distinct groups. In this survey, *G. flavobrunneus* was not encountered, and specimens of *G. liber* and *G. pulcher* were not considered for further analysis. The remaining frogs were categorized into two main groups (Figs 6–8). One group consisted of relatively small-sized specimens with a greenish brown color and variable brown pattern, distinct silvery blotches on the flanks, and relatively indistinct femoral glands in males (Fig. 8). The other group included larger, brown-colored frogs with interrupted light dorsolateral stripes, rather indistinct or absent silvery flank blotches, and distinct brown-orange colored femoral glands in males (Fig. 8). Although these individuals were not sampled, subsequent fieldwork in June and November 2022 yielded additional individuals clearly assignable to these two clusters which genetically belonged to *G.* sp. Ca14 (Fig. 5) and *G.* sp. Ca3 (Fig. 7), respectively. Body size data from the April 2022 field survey specimens indicate statistically significant sexual size dimorphism, with females being larger in *G.* sp. Ca14 (male mean 20.1 mm SVL ± 1.8 SD, n = 37; female mean 21.1 ± 1.6 SD, n = 58; t = -2.792, df = 93, p = 0.006) and in *G.* sp. Ca3 (male mean 23.1 mm SVL ± 1.4 SD, n = 27; female mean 25.7 ± 2.4 SD, n = 51; t = -6.195, df = 76, p < 0.001). Further, *G.* sp. Ca3 individuals were significantly larger than *G.* sp. Ca14 individuals, on average (t = 12.834, df = 171, p < 0.001). Data from the field also hints to a possible difference in sex ratio in April 2022; sex ratios were significantly female biased in both species (*G.* sp. Ca14: 0.627 male/female ratio; $X^2 = 4.642$, df = 1, p = 0.031; *G.* sp. Ca3: 0.529 male/female ratio; $X^2 = 7.385$, df = 1, p = 0.007).

Species delimitation and taxonomic conclusions

As with several other groups of Malagasy frogs, such as the different subgroups of *Mantidactylus* (Scherz *et al.* 2019, 2022) and *Gephyromantis* (Vences *et al.* 2021a; Miralles *et al.* 2023), *Guibemantis* are characterized by a puzzling diversity of deeply divergent mitochondrial lineages, not all of which appear to be reflected in nuclear genomic variation. Nevertheless, the co-occurrence of several of these lineages with distinct morphological and/or bioacoustic differences or without admixture in their nuclear genomes (as with *G. razandry* and *G. razoky*; Koppetsch *et al.* 2023) provides clear evidence that they represent distinct species. In the following, we review the species delimitation evidence for the focal lineages of the present study.

First of all, as summarized in the first section of Results above, all nominal species and candidate species of *Guibemantis* differ from each other by a minimum of 3% uncorrected pairwise distance (mostly >5%), a value that in most cases indicates species-level distinctness in neobatrachian frogs (Fouquet *et al.* 2007; Vieites *et al.* 2009). Furthermore, ASAP suggested all focal lineages as distinct subsets, i.e., as primary species hypotheses (PSH) *sensu* Puillandre *et al.* (2021). For the following focal lineages from the wider Andasibe area, we consider the available species delimitation evidence as sufficient to confirm these PSH as secondary species hypotheses:

(i) *G. pulcher* and *G. flavobrunneus* are characterized by unique morphologies and concordance of morphological and molecular divergences; their species status is therefore beyond doubt. The clade containing these two species plus *G. pulcherrimus* has been taxonomically revised by Vences *et al.* (2023).

(ii) *Guibemantis methueni* is a species primarily occurring at lower elevations in the Northern Central East. Phylogenetically, it likely is sister to *G. woosteri* from the North East of Madagascar according to the most comprehensive multigene tree of Koppetsch *et al.* (2023). Thus, *Guibemantis methueni* is not closely related to the other *Pandanusicola* species occurring in the Andasibe area. *Guibemantis methueni* shares alleles in the RAG-1 fragment studied here with *G. bicalcaratus* and *G.* sp. Ca8 (Fig. 3), but not with any of the other focal lineages. It co-occurs on Nosy Boraha islet with *G. bicalcaratus* and here, the two species have only a very limited amount of haplotype sharing and differ by weak differences in coloration, supporting their species distinctness (Vences *et al.* 2013). From *G.* sp. Ca3, *G.* sp. Ca8 and other focal lineages in the Andasibe area, *G. methueni* differs by its trill (vs. click or chirp) call. We therefore consider *G. methueni* a distinct species.

(iii) *Guibemantis* sp. Ca14 is characterized by a uniquely small body size, as well as a differentiating combination of non-translucent greenish color and a few rather distinct silvery flecks on the posterior flanks; this species has an isolated phylogenetic position in the 16S tree and shares no RAG-1 or SACS haplotypes with its syntopic congeners (Fig. 3). The lineage also differs by its chirp calls from *G. methueni* (trill calls) and from *G.* sp. Ca8 and Ca22 (single-click calls). Therefore, we conclude this lineage represents a highly distinct and unambiguously delimited unnamed species.

(iv) *Guibemantis* sp. Ca3 was included in the multigene phylogenetic analysis of Koppetsch *et al.* (2023) represented by ZCMV 2320 and placed in a clade with three candidate species (here named *G.* sp. Ca11, *G.* sp. Ca23 and *G.* sp. Ca24). According to the 16S tree herein (Fig. 1), also *G. bicalcaratus*, *G.* sp. Ca8 and *G.* sp. Ca22 probably belong to the same clade. Morphologically, the brown dorsal color with distinct interrupted light dorsolateral bands typical for *G.* sp. Ca3 distinguishes it from all other *Pandanusicola* species known from the Andasibe area except *G.* sp. Ca22 (for which color is not reliably known), and also from other brown-colored *Guibemantis* including *G. bicalcaratus.* Bioacoustically, it is characterized by single-click calls, but comparative advertisement call data among the related species are only known for *G.* sp. Ca8 (which has a shorter note duration). The networks of the nuclear markers illustrate a lack of haplotype sharing of *G.* sp. Ca3 with *G. methueni*, *G.* sp. Ca8, *G.* sp. Ca14, and also (for RAG-1 only) with *G. bicalcaratus* (Fig. 3). Haplotype sharing in SACS is observed with *G. wattersoni*, but this species phylogenetically belongs to a distant clade within *Pandanusicola* (Koppetsch *et al.* 2022). The combined evidence supports *G.* sp. Ca3 as distinct evolutionary lineage meriting species status. Extensive haplotype sharing in both nuclear markers is however observed with *G.* sp. Ca22 which therefore may be conspecific with *G.* sp. Ca3.

(v) Finally, *G.* sp. Ca8 likely belongs into the same clade within *Pandanusicola* as *G.* sp. Ca3 (Fig. 1). Compared to other lineages in this clade, it lacks haplotype sharing in SACS and RAG-1 with *G.* sp. Ca3, and in RAG-1 with *G. bicalcaratus* (Fig. 3). In RAG-1, haplotype sharing is observed with *G. methueni*, but from this species it differs by a distant phylogenetic position, click vs. trill advertisement calls, and more contrasted color of femoral glands. *Guibemantis* sp. Ca8 further differs from *G.* sp. Ca3 by shorter note duration in calls and absence of contrasted light dorsolateral bands. We therefore conclude that *G.* sp. Ca8 represents a distinct species as well.

Consequently, in the following we formally name, diagnose, and describe three new species of *Guibemantis* (*Pandanusicola*), corresponding to the mitochondrial lineages provisionally named *G.* sp. Ca14, *G.* sp. Ca3, and *G.* sp. Ca8.

Species accounts

Guibemantis rianasoa sp. nov.

(Figs 6, 7, 12)

Remark. This species has not been reported from Andasibe in previous publications, but based on a specimen from Fierenana, it was named *Guibemantis* sp. aff. *punctatus* "Fierenana" in Glaw & Vences (2007), *G.* sp. 14 in Vieites *et al.* (2009) and *G.* sp. Ca14 in Perl *et al.* (2014).

Holotype. ZSM 149/2022 (field number ZCMV 13705), adult male, collected by M. Vences, S. Rakotomanga, S. Rasamison, and P. Galán on 17–18 November 2022 at Andasibe, VOI (VOIMMA) forest, central eastern Madagascar, approximate coordinates -18.9277, 48.4186, ca. 950 m above sea level.

Paratypes. Five specimens: ZSM 148/2022 (ZCMV 13704), adult male, same collection data as holotype; ZSM 150/2022 (ZCMV 15636), ZSM 151/2022 (ZCMV 15637), UADBA-ZCMV 15633, and UADBA-ZCMV 15634, four adults (probably females) collected by A. Rakotoarison on 14–15 June 2022 in the Andasibe area.

Definition. Assigned to the subgenus *Pandanusicola* in the genus *Guibemantis* based on its small body size, phytotelm-dwelling habitats (in *Pandanus* plants), near-absent webbing between toes, connected lateral metatarsalia, presence of both inner and outer metatarsal tubercles, intercalary elements between ultimate and penultimate phalanges of fingers and toes (verified by external examination), presence of femoral glands in males (absent in females) consisting of well-delimited (though poorly recognizable) femoral macroglands with discrete enlarged gland granules and without externally visible central depression, and presence of whitish color laterally on throat (marking the vocal sac) in males (absence in females), and molecular phylogenetic affinities.

The new species is characterized by the unique combination of: (1) small size, with adult male SVL up to 20 mm in genotyped individuals (possibly up to an exceptional 27 mm according to field data from non-genotyped individuals), (2) dull greenish (not bright translucent green) dorsally, without purplish spots, (3) distinct brown rostral stripe, (4) presence of a few rather distinctly contrasted white-silvery flecks on the posterior flanks, (5) often copper-golden color above the eyes, (6) absence of webbing on hand and only traces of web at foot, (6) vomerine teeth present, (7) femoral (macro)glands of males small and poorly marked.

FIGURE 6. *Guibemantis rianasoa* **sp. nov.** (sp. F / Ca14), color variation in life. All pictured specimens were photographed at Andasibe and were not collected or genotyped. Note presence of rather distinct silvery flank blotches in all specimens pictured in lateral view.

Although some individuals with atypical coloration may be difficult to distinguish from subadults of other *Pandanusicola* species, *G. rianasoa* is overall rather easily diagnosable, and it does not appear to have clear phylogenetic affinities to other species. The species is also characterized by numerous diagnostic nucleotide positions in the mitochondrial 16S rRNA gene: MolD identified a robust diagnostic nucleotide combination of an 'A' in the site 1203, 'T' in the site 1307, 'A' in the site 1329 (positions relative to the full 16S rRNA gene of *Mantella madagascariensis*).

Diagnosis. Distinction from *G. fotsitenda, G. liber, G. razandry, G. razoky* and *G. tasifotsy*: male femoral gland consisting of a well-delimited field of discrete enlarged single gland granules (vs. a diffuse field of small granules covering most of the ventral shank), occurrence limited to *Pandanus* leaf axils (vs. calling and breeding in open swamps), and low-intensity calls emitted from *Pandanus* vs. loud calls emitted from exposed perches above swamps.

Distinction from *G. albolineatus*: greenish dorsal color (vs. almost uniformly chocolate-brown), presence of silvery white dots on flanks (vs. absence), and absence of contrasted and well-delimited light dorsolateral bands (vs. presence).

Distinction from *G. albomaculatus*: smaller body size (male SVL ≤20 mm vs. >20 mm in the majority of specimens), absence of fine white dotting on body (vs. presence especially on hindlimbs and sometimes on dorsum), presence of silvery white dots on flanks (vs. absence), and small and inconspicuously colored femoral glands (vs. larger and with contrasting yellowish color).

Distinction from *G. annulatus*: smaller body size (male SVL ≤20 mm vs. >20 mm), olive greenish dorsal color (vs. light brownish), absence of small dark dots dorsally (vs. presence), presence of silvery white dots on flanks (vs. absence), and absent or poorly contrasted light ring proximal to finger and toe discs (vs. distinct and contrasted).

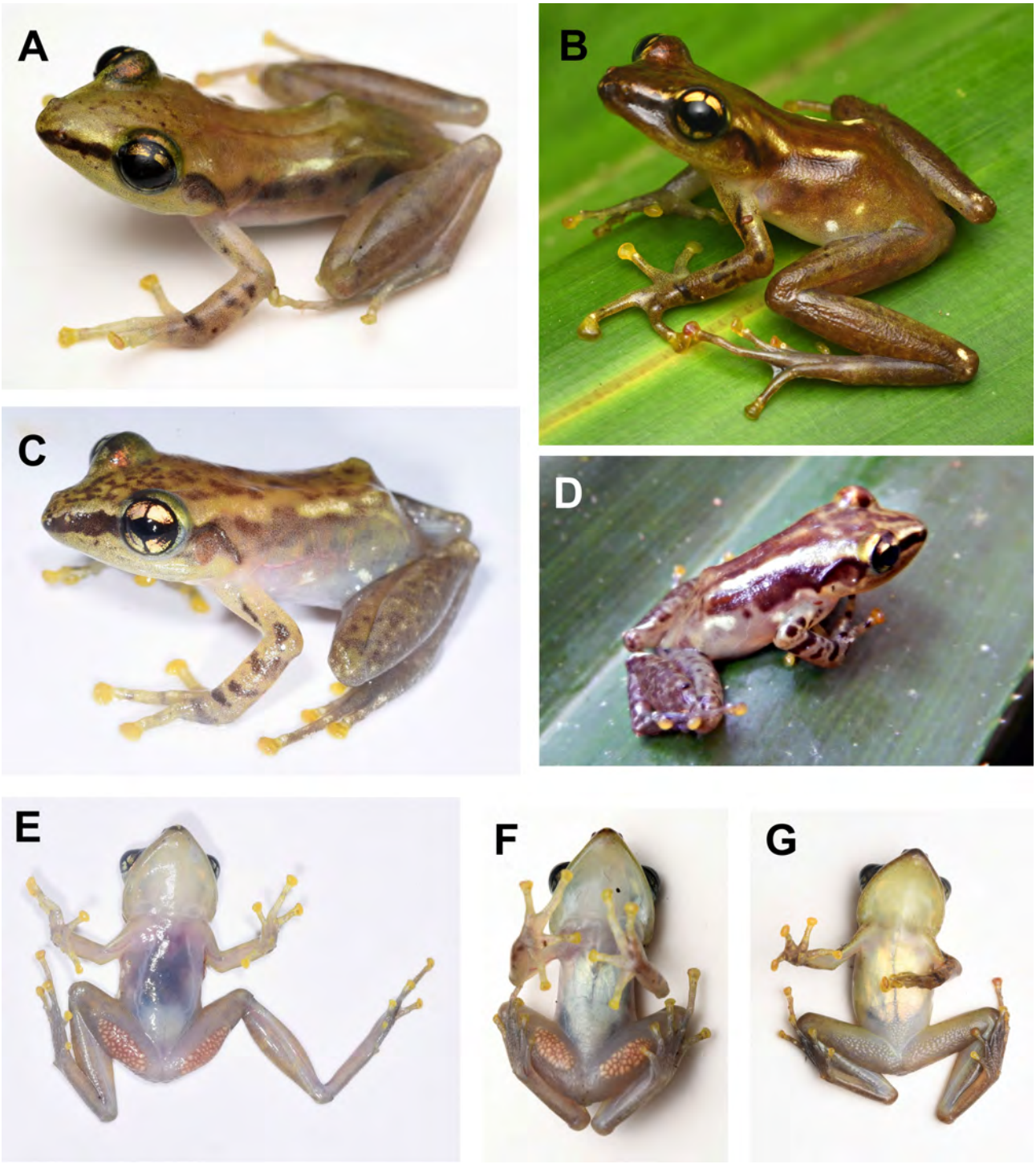

FIGURE 7. *Guibemantis ambakoana* **sp. nov.** (sp. A / Ca3) in life. **A, F.** Male holotype ZSM 152/2022 (ZCMV 13707) from Andasibe VOI forest; **B, G.** Female paratype ZSM 153/2022 (ZCMV 13717) also from Andasibe VOI forest; **C, E.** Male paratype ZSM 431/2016 (ZCMV 15001) from Andasibe (Analamazaotra forest); **D.** UADBA-ZCMV 15635 from Andasibe. Note the distinct femoral glands with orange tint present in male specimens.

Distinction from *G. bicalcaratus*: smaller body size (male SVL ≤20 mm vs. >20 mm), presence of a black vertical line in upper part of iris (vs. absence), olive greenish dorsal color (vs. light brownish), and presence of silvery white dots on flanks (vs. absence).

Distinction from *G. flavobrunneus*: much smaller body size (male SVL ≤20 mm vs. ≥30 mm), presence of silvery white dots on flanks (vs. absence), and an olive greenish dorsal color (vs. brown with contrasted light brown pattern).

Distinction from *G. methueni*: smaller body size (male SVL ≤20 mm vs. >20 mm), olive greenish dorsal color (vs. light brownish), presence of silvery white dots on flanks (vs. absence), and males with white color only laterally on throat (vs. white color covering most of throat).

Distinction from *G. milingilingy*: smaller body size (male SVL ≤20 mm vs. >20 mm), presence of silvery white dots on flanks (vs. absence), and small and inconspicuously colored femoral glands (vs. larger and with contrasting yellowish color).

Distinction from *G. pulcher* and *G. pulcherrimus*: smaller body size (male SVL ≤20 mm vs. >20 mm in almost all specimens), non-translucent greenish dorsal color (vs. translucent green), absence of purple-reddish dots and markings on the dorsum (vs. presence), and small inconspicuously colored femoral glands (vs. larger and with contrasting yellowish color).

Distinction from *G. punctatus*: smaller body size (male SVL ≤20 mm vs. >20 mm in the majority of specimens), olive greenish dorsal color (vs. light brownish), presence of silvery white dots on flanks (vs. absence), and absence of small dark dots dorsally (vs. presence).

Distinction from *G. wattersoni*: smaller body size (male SVL ≤20 mm vs. >20 mm), olive greenish dorsal color (vs. light brownish), and presence of silvery white dots on flanks (vs. absence).

Distinction from *G. woosteri*: smaller body size (male SVL ≤20 mm vs. >20 mm in almost all specimens), and presence of silvery white dots on flanks (vs. absence).

Description of the holotype. Adult male in good state of preservation (Fig. 11). Tissue removed from ventral side of right thigh for DNA extraction. Head longer than wide and slightly wider than body; snout slightly pointed in dorsal and ventral views, more rounded in lateral view; canthus rostralis straight, loreal region flat; nostrils much nearer to tip of snout than to eye, tympanum distinct, 43% of horizontal eye diameter; supratympanic fold distinct, curved; vomerine odontophores small but distinct, located medially between eye and choanae on either side of head; maxillary teeth present; tongue ovoid, and distinctly bifid at its tip. Arms slender; relative finger length 1<2<4<3, second finger very slightly shorter than fourth finger; finger discs moderately enlarged and squared off at tips in a rounded 'T' shape, no webbing between fingers recognizable, subarticular tubercles distinct, unpaired. Hindlimbs moderately slender, foot length 82% of tibia length; lateral metatarsalia largely connected by muscular tissue; inner metatarsal tubercle oblong and recognizable, relatively small; outer metatarsal tubercle round, small and distinct; only traces of webbing recognizable between toes, especially toes 3, 4 and 5; relative length of toes 1<2<5<3<4, third toe slightly longer than fifth; toe discs moderately enlarged. Femoral glands visible but not very prominent. For morphometric measurements see Table 1.

After ca. four months in preservative (Fig. 11), dorsal surface is beige and mottled gray-green starting at the cloaca and stopping between the eyes. Beige dorsolateral bands present but not continuous, from sacral vertebrae bump up to the eyes. Rostral stripe is black and distinctly delimited, continues onto supratympanic fold before stopping at the forelimb insertion. Anterior flanks each marked with small and asymmetric white patches. Forelimbs and hindlimbs are beige with gray-green stripes, stripes are less distinct on hindlegs. Toe discs yellow. Ventral side beige, with faint black stippling visible on the underside of the hands, feet and thighs. In life, dorsal surface was greenish (of rather dull, only slightly translucent appearance, clearly less translucent than is typical for *G. pulcher*) with faint mottling, transitioning to pale blueish on the hindlimbs and featuring asymmetric silver patches on the flanks (Fig. 5).

Variation. Some frogs found in Andasibe have a blue tint towards the posterior parts of the body, and while the base green coloring remains relatively constant across specimens, a dark brown asymmetrical mottled secondary color is highly variable (Figs 6–7). The dark brown secondary coloration can range from highly translucent to nearly black, usually concentrated on the flanks and towards the cloaca, but sometimes covering the entire specimen. Silver blotches on the flanks vary in size and shape but are usually distinct. Femoral glands of males are only weakly expressed and of the same color as the surrounding skin ventrally on thigh. Males only with a little amount of white color laterally on the throat (absent in females), and slightly smaller than females (SVL 18–27 mm in males, 19–26 mm in females, but only 12 out of 95 individuals >23 mm; see section "Morphological differentiation" above). The

TABLE 1. Morphometric measurements (all in mm) of genotyped adults of species of *Guibemantis* targeted in this study. For abbreviations of measurements, see Materials and Methods; other abbreviations: HT, holotype; PT, paratype; M, male; F, female.

Catalogue number	Field number	Locality	Status	Sex	SVL	HW	HL	TD	ED	END	NSD	NND	FORL	HAL	HIL	FOTL	FOL	TIBL	FGL	FGW
G. rianasoa **sp. nov.** (F)																				
ZSM 149/2022	ZCMV 13705	Andasibe	HT	M	19.1	6.7	7.7	1.2	2.8	2.0	1.3	2.0	12.0	5.3	30.0	12.8	8.0	9.6	3.9	1.5
ZSM 148/2022	ZCMV 13704	Andasibe	PT	M	19.9	6.6	8.0	1.2	3.0	2.1	1.0	1.7	12.5	5.5	30.4	14.6	8.3	9.8	3.5	1.6
UADBA	ZCMV 15633	Andasibe	PT	F	20.1	6.7	8.8	1.3	2.6	2.1	1.8	2.1	13.1	5.9	31.5	13.8	9.0	10.2		
UADBA	ZCMV 15634	Andasibe	PT	F	21.4	7.3	8.3	1.5	3.0	2.3	1.7	2.4	12.8	6.0	31.2	13.6	8.4	9.8		
ZSM 150/2022	ZCMV 15636	Andasibe	PT	F	21.2	7.1	8.0	1.8	2.9	2.4	1.5	2.3	13.1	6.5	30.8	14.3	8.6	10.5		
ZSM 151/2022	ZCMV 15637	Andasibe	PT	F	21.3	6.9	7.7	1.4	2.9	2.3	1.8	2.4	13.4	6.2	31.7	14.3	8.9	10.4		
G. ambakoana **sp. nov.** (A)																				
ZSM 152/2022	ZCMV 13707	Andasibe	HT	M	23.7	7.7	9.3	1.8	3.6	2.4	1.3	2.1	14.3	7.1	37.4	16.9	10.8	12.1	5.1	1.9
ZSM 431/2016	ZCMV 15001	Andasibe	PT	M	22.6	7.6	9.1	1.8	2.9	2.5	1.2	1.8	14.0	6.0	35.0	15.5	9.6	11.4	5.7	2.0
ZSM 275/2016	FGZC 5296	S Moramanga	PT	M	24.0	8.1	9.5	2.0	3.8	2.2	1.7	2.5	15.6	7.3	36.7	17.4	11.0	12.3	5.4	1.9
ZSM 153/2022	ZCMV 13717	Andasibe	PT	F	23.7	8.5	9.6	1.8	3.5	2.3	1.4	2.0	15.5	7.3	39.0	16.9	10.6	12.9		
ZSM 432/2016	ZCMV 15002	Andasibe	PT	F	26.0	9.0	11.1	2.2	3.6	2.8	1.6	2.3	16.3	7.8	48.5	17.4	10.8	12.8		
UADBA	ZCMV 15635	Andasibe	PT	F	25.4	8.5	9.4	2.3	3.6	2.8	1.8	2.4	15.0	7.6	39.0	17.1	11.2	12.9		
ZSM 156/2022	ZCMV 15638	Andasibe	PT	F	28.3	9.5	10.9	2.2	3.7	2.8	1.6	2.5	16.5	7.7	41.3	18.8	11.8	13.6		
UADBA	ZCMV 15631	Andasibe	PT	F	22.8	7.4	9.3	2.0	3.5	2.4	1.5	2.6	14.3	7.0	35.0	16.6	10.1	11.8		

.....Continued on the next page

TABLE 1. (Continued)

Catalogue number	Field number	Locality	Status	Sex	SVL	HW	HL	TD	ED	END	NSD	NND	FORL	HAL	HIL	FOTL	FOL	TIBL	FGL	FGW
ZSM 154/2022	ZCMV 13718	Andasibe	PT	F	24.6	8.6	10.3	2.1	3.6	2.5	1.5	2.4	15.4	7.2	40.6	18.3	11.4	13.0		
G. cf. *ambakoana* **sp. nov.** (E)																				
	ZCMV 15632	Andasibe		F	23.7	8.0	9.5	1.7	3.6	2.4	1.7	2.3	14.7	6.7	37.4	17.1	10.5	12.2		
G. vakoa **sp. nov.** (C)																				
ZSM 389/2004	ZCMV 931	Besariaka	HT	M	23.6	8.0	9.6	1.6	3.7	3.0	1.5	2.4	14.6	7.2	34.1	16.3	10.2	11.1	5.0	2.1
ZSM 388/2004	ZCMV 930	Besariaka	PT	M	23.0	8.1	10.0	2.0	3.6	2.6	1.7	2.4	15.0	7.3	37.3	17.1	10.1	11.7	5.0	2.2
G. methueni																				
ZSM 3223/2012	ZCMV 14089	Andasibe		M	23.2	8.4	9.9	1.8	3.7	2.8	1.8	2.5	12.4	6.5	33.0	34.8	9.6	11.4	5.8	2.1

only known specimen from Fierenana has a substantial divergence in its 16S sequence (3.0% to Andasibe samples) and also shows differences in coloration in life, with a somewhat vermiculated dark pattern evenly distributed not only on the dorsum but also on the flanks.

Etymology. The species epithet is derived from the Malagasy words *riana* (waterfall) and *soa* (beautiful), making reference to the greenish (somewhat greenish blue) color of the species with silvery blotches which remind colors of water reflecting forest vegetation. The name also makes reference to the "Rianasoa trail" in Mantadia National Park where we have observed the species. The name is used as a noun in apposition.

Natural history. Specimens were observed exclusively in *Pandanus* plants during the day. Of 253 *Pandanus* surveyed by HG in 2022, *G. rianasoa* was detected in 136 plants (53.7%) and co-occurred in syntopy with *G. ambakoana* in 76 plants (30.0%). Clutches observed in the *Pandanus* leaf axils could not be assigned to any of the various species occurring in syntopy as they were not genotyped. No further natural history or life history data are known.

Bioacoustics. Vocalizations were recorded in Analamazaotra Forest Station in the Andasibe area at 11:16 h during a period of light rain, at an air temperature of 19–21°C. The call (Fig. 4A) was recorded from ca. two meters distance close to a path in secondary humid forest. Notably, the calling individual was visually identified as *Guibemantis rianasoa* **sp. nov.** in the field and observed and videotaped, but the frog was not collected as a voucher and not sequenced. The following call description therefore cannot be attributed to this species with absolute certainty. Advertisement calls are rather soft and consist of a single very short pulsatile note, emitted at regular intervals within short call series containing two calls (Fig. 4A). Amplitude modulation is evident in each call, with maximum call energy present at the beginning of the call, slowly decreasing towards the call's end. The initial call of each call series exhibits less call energy and has a lower dominant frequency when compared to the second calls of series. Numerical parameters of eight analyzed calls from two individuals are as follows: call duration (= note duration) 7–15 ms (10.8 ± 2.9 ms); inter-call intervals within call series 128–149 ms (138.5 ± 8.7 ms); number of calls per call series 2; duration of call series 151–171 ms (159.8 ± 8.4 ms); dominant frequency 3391–5071 Hz (4239 ± 784 Hz); prevalent bandwidth 2400–9400 Hz. Call repetition rate within call series was approximately 400 calls/minute.

Advertisement calls recorded on 19 November 2022 at Andasibe (air temperature not measured) are in general agreement with those described above, being rather soft and consisting of a single very short pulsatile note, emitted at regular intervals within short call series containing 2–3 calls. No vouchers were collected for these calls, but they were regularly heard from *Pandanus* plants in which only this species was found. Numerical parameters of 23 analyzed calls from at least two individuals are as follows: call duration (= note duration) 8–24 ms (13.4 ± 4.0 ms); inter-call intervals within call series 115–195 ms (132.3 ± 23.6 ms); number of calls per call series 2–3 (2.1 ± 0.4); duration of call series 147–232 ms (191.5 ± 58.4 ms); dominant frequency 3413–5092 Hz (4267 ± 545 Hz); prevalent bandwidth 2500–6500 Hz. Call repetition rate within call series was approximately 400 calls/minute.

Distribution. The species is so far only known from (1) the area around Andasibe and (2) Fierenana. At Andasibe, it has been found in the VOI forest, at Analamazaotra Forest Station, and within Analamazaotra-Mantadia National Park (Figs 1–2).

***Guibemantis ambakoana* sp. nov.**
(Figs 8, 9, 12)

Remark. Individuals probably belonging to this species have been reported as *Guibemantis bicalcaratus* and *G. albolineatus* in Glaw & Vences (1994), *G.* cf. *albolineatus* in Lehtinen *et al.* (2007), *G.* sp. aff. *albolineatus* "Andasibe" in Glaw & Vences (2007), *G.* sp. 3 in Vieites *et al.* (2009) and *G.* sp. Ca3 in Perl *et al.* (2014).

Holotype. ZSM 152/2022 (ZCMV 13707), adult male, collected by M. Vences, S. Rakotomanga, S. Rasamison, and P. Galán on 17–18 November 2022 at Andasibe, VOI (VOIMMA) forest, central eastern Madagascar, approximate coordinates -18.9277, 48.4186, ca. 950 m above sea level.

Paratypes. Seven specimens. ZSM 153/2022 (ZCMV 13717) and ZSM 154/2022 (ZCMV 13718), two adult females with same collection data as holotype; ZSM 156/2022 (ZCMV 15638), UADBA-ZCMV 15635 and UADBA-ZCMV 15631, three females collected by A. Rakotoarison, A.I.F. Hasiniaina and E. Desire on 14–15 June 2022 in the Andasibe area; ZSM 275/2016 (FGZC 5296), adult male, collected by F. Glaw, D. Prötzel, J. Forster, N. Raharinoro on 3 August 2016 south of Moramanga at geographical coordinates -19.06155, 48.23205, 962 m a.s.l.;

ZSM 431/2016 (ZCMV 15001) and ZSM 432/2016 (ZCMV 15002), one male and one female, collected by M. Vences on 10 November 2016 in the Analamazaotra Forest Station ("Mitsinjo Forest", ca. -18.934, 48.410).

Referred specimen. ZSM 155/2022 (ZCMV 15632), one female of mitochondrial lineage E, collected by A. Rakotoarison, A.I.F. Hasiniaina and E. Desire on 14–15 June 2022 in the Andasibe area.

Definition. Assigned to the subgenus *Pandanusicola* in the genus *Guibemantis* based on its small to medium body size, phytotelm-dwelling habitats (in *Pandanus* plants), near-absent webbing between toes, connected lateral metatarsalia, presence of both inner and outer metatarsal tubercles, intercalary elements between ultimate and penultimate phalanges of fingers and toes (verified by external examination), presence of well-delimited femoral macroglands consisting of discrete enlarged gland granules and without externally visible central depression, and of whitish color laterally on throat (marking the vocal sac) in males (absence in females), and molecular phylogenetic affinities.

The new species is characterized by the combination of the following characters: (1) small size with adult SVL up to 24 mm in males and up to 28 mm in females in genotyped individuals (up to 27 mm / 30 mm based on field measurements of non-genotyped individuals), (2) light brownish dorsal color, often without distinct darker markings or spots, (3) distinct brown rostral stripe, (4) no or only few, small whitish spots on (posterior) flanks, (5) often with incomplete or interrupted light brown, beige or yellowish dorsolateral stripes, (6) absence of webbing on hand and only traces of web at foot, (7) vomerine teeth present, (8) femoral (macro)glands of males distinct, very clearly recognizable and of contrasting reddish brown color in life, single gland granules well recognizable externally in life and preservative.

Although this combination of character states will allow a distinction from most other species of *Guibemantis*, especially the co-occurring *G. flavobrunneus, G. pulcher,* and *G. rianasoa*, it is more difficult to diagnose the species against other brownish-colored species such as *G. albolineatus, G. bicalcaratus, G. methueni,* or *G. wattersoni*. Furthermore, we here restrict the type series of this species to individuals belonging to mitochondrial lineage A, and their morphological diagnosis from lineage E is unclear. Thus, we define this species based on diagnostic nucleotide positions (typical for lineage A) in the mitochondrial 16S rRNA gene; MolD identified a robust diagnostic nucleotide combination of a 'T' in the site 1091, 'A' in the site 1108, 'A' in the site 1129, 'T' in the site 1134 (positions relative to the full 16S rRNA gene of *Mantella madagascariensis*).

Diagnosis. Distinction from *G. fotsitenda, G. liber, G. razandry, G. razoky* and *G. tasifotsy*: male femoral gland consisting of a well-delimited field of discrete enlarged single gland granules (vs. a diffuse field of small granules covering most of the ventral shank), occurrence limited to *Pandanus* leaf axils (vs. calling and breeding in open swamps), and calls emitted from *Pandanus* vs. loud calls emitted from exposed perches above swamps.

Distinction from *G. albolineatus*: contrasted and well-delimited dorsolateral bands that are typically interrupted or present only on the central dorsum (vs. dorsolateral bands continuous).

Distinction from *G. albomaculatus*: absence of fine white dotting on body (vs. presence, especially on hindlimbs and sometimes on dorsum), males with white color only laterally on throat (vs. white color covering most of throat), and presence of well-delimited dorsolateral bands that are typically interrupted or present only on the central dorsum (vs. absent or poorly contrasted but continuous).

Distinction from *G. annulatus*: absence of a regular pattern of small dark dots dorsally (vs. presence), and absent or poorly contrasted light ring proximal to finger and toe discs (vs. distinct and contrasted).

Distinction from *G. bicalcaratus*: presence of well-delimited dorsolateral bands that are typically interrupted or present only on the central dorsum (vs. absence), and presence of a black vertical line in upper part of iris (vs. absence).

Distinction from *G. flavobrunneus*: smaller body size (male SVL 23–24 mm vs. ≥30 mm), and dorsum brown with well-delimited dorsolateral bands that are typically interrupted or present only on the central dorsum (vs. brown with contrasted light brown pattern).

Distinction from *G. methueni*: presence of well-delimited dorsolateral bands that are typically interrupted or present only on the central dorsum (vs. absent or poorly contrasted but continuous), femoral glands typically with contrasting yellow-orange color (vs. without contrasting color), and males with white color only laterally on throat (vs. white color covering most of throat).

Distinction from *G. milingilingy*: presence of well-delimited dorsolateral bands that are typically interrupted or present only on the central dorsum (vs. broader and continuous), and dorsal color brown typically without greenish shade (vs. yellowish green dorsolateral bands and dorsal markings).

Distinction from *G. pulcher* and *G. pulcherrimus*: brown dorsal color (vs. translucent green), and absence of purple-reddish dots and markings on the dorsum (vs. presence).

Distinction from *G. punctatus*: absence of a regular pattern of small dark dots dorsally (vs. presence), and presence of well-delimited dorsolateral bands that are typically interrupted or present only on the central dorsum (vs. absence).

Distinction from *G. rianasoa*: larger body size (male SVL 23–24 mm vs. ≤20 mm), brown dorsal color (vs. olive greenish), and large femoral glands with contrasting yellowish color in males (vs. small and inconspicuously colored).

FIGURE 8. Color variation in life in specimens assigned to *Guibemantis ambakoana* **sp. nov.** (sp. A / Ca3). All pictured specimens were photographed at Andasibe and were not collected or genotyped, and may therefore include both mitochondrial lineages A and E. Note absence of silvery flank blotches and distinct femoral glands with orange tint in the two male specimens pictured in ventral view.

Distinction from *G. wattersoni*: presence of well-delimited dorsolateral bands that are typically interrupted or present only on the central dorsum (vs. absent or poorly contrasted but continuous).

Distinction from *G. woosteri*: presence of well-delimited dorsolateral bands that are typically interrupted or present only on the central dorsum (vs. absent or poorly contrasted but continuous), and a brown dorsal color without greenish elements (vs. often a green shade, especially of dorsolateral bands).

Description of the holotype. Adult male in good state of preservation (Fig. 11). Tissue removed from ventral side of right thigh for DNA extraction. Head longer than wide and wider than body; snout pointed in dorsal and ventral views, more rounded in lateral view; canthus rostralis straight, loreal region flat; nostrils much nearer to tip of snout than to eye, tympanum distinct, 50% of horizontal eye diameter; supratympanic fold distinct, curved; vomerine odontophores small but distinct, located medially between eye and choanae on either side of head; maxillary teeth present; tongue ovoid, and distinctly bifid at its tip. Arms slightly slender; relative finger length 1<2<4<3, second finger very slightly shorter than fourth finger; finger discs moderately enlarged and squared off at tips in a rounded 'T' shape, no webbing between fingers recognizable, subarticular tubercles distinct, unpaired. Hindlimbs moderately slender, foot length 89% of tibia length; lateral metatarsalia largely connected by muscular tissue; inner metatarsal tubercle oblong and recognizable, relatively small; outer metatarsal tubercle round, small and distinct; only traces of webbing recognizable between toes; relative length of toes 1<2<5<3<4, third toe slightly shorter than fifth; toe discs moderately enlarged. Femoral glands distinct and prominent. For morphometric measurements see Table 1.

After ca. four months in preservative (Fig. 11), dorsal surface gray. Beige dorsolateral bands are faint and appear next to a distinct dark brown rostral stripe which stretches from the tip of the nose all the way along the anterior flanks, stopping at the hindleg insertion. A thin, vertical, straight line of maroon tint is visible in the center of the dorsal view. Tiny dots between the eyes and towards the snout. Forelimbs gray with dark brown discontinuous stripes, hindlegs gray, speckled with light brown. Ventral side beige, with faint black stippling on the underside of hands, feet, hindlegs, and around the mouth. In life (Fig. 7), dorsal surface was golden brown, with a dark brown rostral stripe, and limbs were pale brown.

Variation. Variation is most obvious in the ground color of the frog, ranging from a pale, mottled beige to chocolate-brown (Figs 8–9). Golden dorsolateral bands, usually present, ranging from continuous and clearly delimited, to patchy and small. Silver patches on the flanks are often present, but not always, and vary in size and shape, usually less contrasted than in *G. rianasoa*. Femoral glands are orange-brown, with distinct and clearly recognizable single gland granules inside the macrogland. Males only with a little amount of white color laterally on the throat (absent in females), and slightly smaller than females (field SVL measurements of non-genotyped individuals 20–27 mm in males, 20–30 mm in females; see section "Morphological differentiation" above).

Etymology. The species epithet is derived from the Malagasy word "vakoana", used to refer to *Pandanus* screw pines; "am-bakoana" means "living in vakoana", and refers to the species' specialized habitat, living and reproducing in *Pandanus* leaf axils. The name is used as a noun in apposition.

Natural history. Specimens were observed exclusively in *Pandanus* plants. Calling males were observed in November 2022 sitting exposed on *Pandanus* leaves, during the day. Of 253 *Pandanus* surveyed by HG in 2022, *G. ambakoana* was detected in 103 plants (40.7%) and co-occurred in syntopy with *G. rianasoa* in 76 plants (30.0%). Nothing else is known.

Bioacoustics. Advertisement calls recorded on 16 November 2013 at Torotorofotsy (air temperature not recorded; call voucher not collected but agreeing in color pattern with this species) consist of a single short pulsatile note, emitted at long somewhat irregular intervals. Amplitude modulation is evident in each call, with maximum call energy present in the first quarter of the call, rapidly decreasing to a much lower level and further gradually fading towards the call's end. Numerical parameters of 52 analysed calls are as follows: call duration (= note duration) 20–41 ms (31.3 ± 7.2 ms); inter-call intervals 1190–2520 ms (1826.7 ± 439.5 ms); dominant frequency 3156–3979 Hz (3629 ± 292 Hz); prevalent bandwidth 2200–5200 Hz. Call repetition rate was approximately between 23–48 calls/minute. Within the recordings, sometimes two calls were emitted in fast succession, with inter-call intervals ranging between 98–155 ms (122.7 ± 120.6 ms). It is unknown if these 'double clicks' are a regular part of the advertisement call, or possibly have another function (e.g. territorial).

Advertisement calls recorded on 19 November 2022 at Andasibe (air temperature not measured; one individual seen calling; Fig. 4B) generally agree in character with those recorded at Torotorofotsy, except for being somewhat longer in duration. Numerical parameters of 43 analysed calls from at least two individuals are as follows: call duration (= note duration) 31–93 ms (63.4 ± 18.1 ms); inter-call intervals 780–2055 ms (1686.6 ± 381.4 ms);

dominant frequency 3262–4124 Hz (3704 ± 278 Hz); prevalent bandwidth 2400–5000 Hz. Call repetition rate was approximately between 25–65 calls/minute.

Distribution. The species is known from (1) the type locality Andasibe, as well as two sites in the same general area of the Northern Central East of Madagascar, i.e., from forest fragments near (2) Moramanga, and (3) Anosibe An'Ala (Figs 1–2). A specimen from Maharira in Ranomafana National Park is genetically highly divergent and is only tentatively assigned to this species (see Fig. 1).

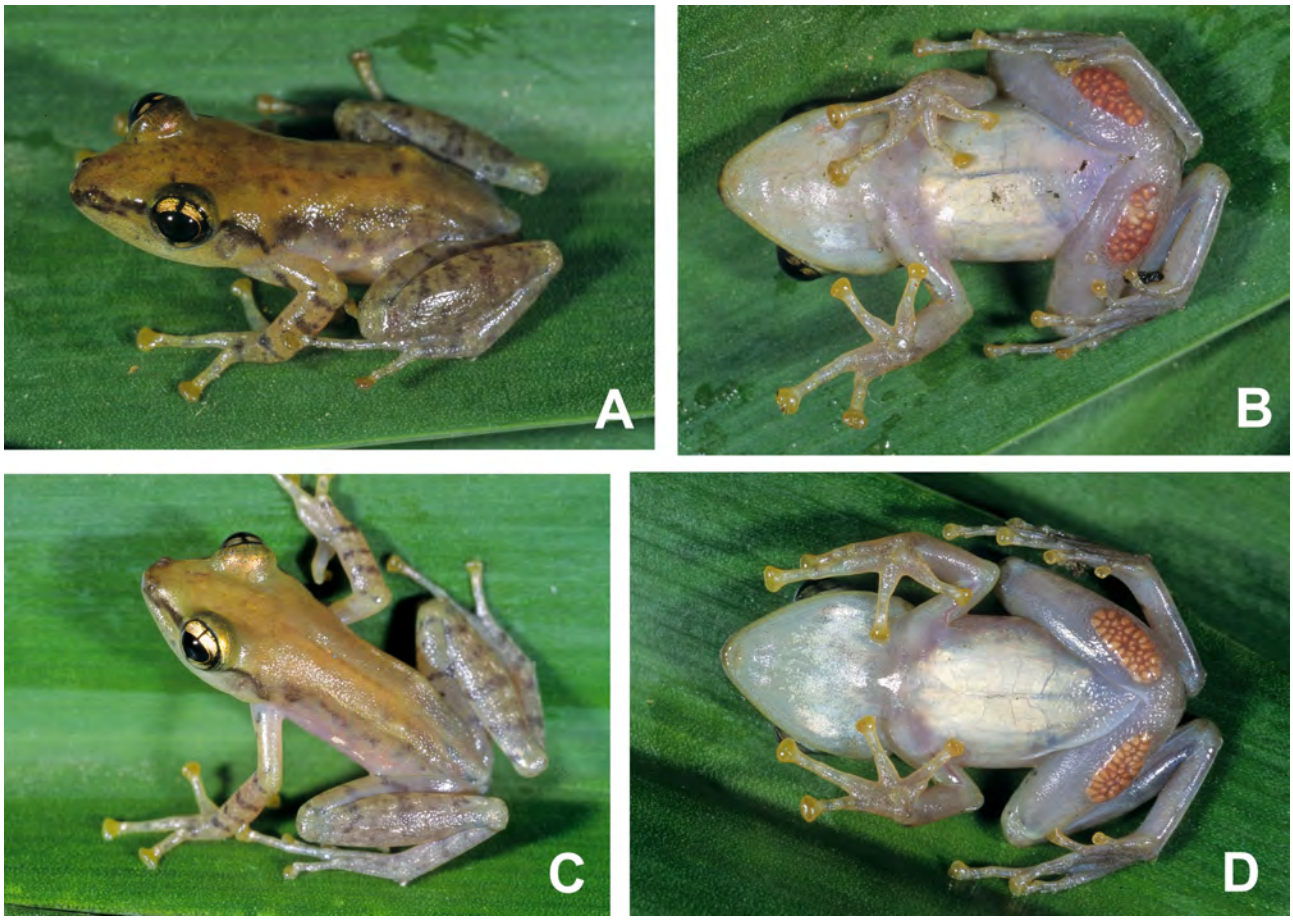

FIGURE 9. Male individuals of *Guibemantis vakoa* **sp. nov.** from Besariaka (south of Moramanga), photographed in 2004. (**A–B**) Holotype ZSM 389/2004 (ZCMV 931). (**C–D**) Paratype ZSM 388/2004 (ZCMV 930) (assigned to species based on morphology only). Note the distinct orangish-brown femoral glands and only limited white throat pigmentation in comparison to syntopic specimens of *G. methueni* which have less distinctly pigmented glands and extended white throat color (Fig. 10).

***Guibemantis vakoa* sp. nov.**
(Figs 10, 12)

Remark. Individuals of this species have been reported as *Guibemantis* sp. aff. *bicalcaratus* "Moramanga" by Glaw & Vences (2007), and as *G.* sp. 8 in Vieites *et al.* (2009) and *G.* sp. Ca8 in Perl *et al.* (2014), but with incorrect field number information for the sample used therein (reported erroneously as ZCMV 466).

Holotype. ZSM 389/2004 (ZCMV 931), adult male, collected by M. Vences, E. Edwards and C. Woodhead on 15 February 2004 at Besariaka (south of Moramanga), central eastern Madagascar, coordinates -19.12863, 48.28063, 976 m a.s.l.

Paratype. One specimen, ZSM 388/2004 (ZCMV 930), adult male with same collection data as holotype.

Definition. Assigned to the subgenus *Pandanusicola* in the genus *Guibemantis* based on its small to medium body size, phytotelm-dwelling habitats (in *Pandanus* plants), near-absent webbing between toes, connected lateral metatarsalia, presence of both inner and outer metatarsal tubercles, intercalary elements between ultimate and penultimate phalanges of fingers and toes (verified by external examination), presence of well-delimited femoral

macroglands consisting of discrete enlarged gland granules and without externally visible central depression and of whitish color laterally on throat (marking the vocal sac) in males (absence in females), and molecular phylogenetic affinities.

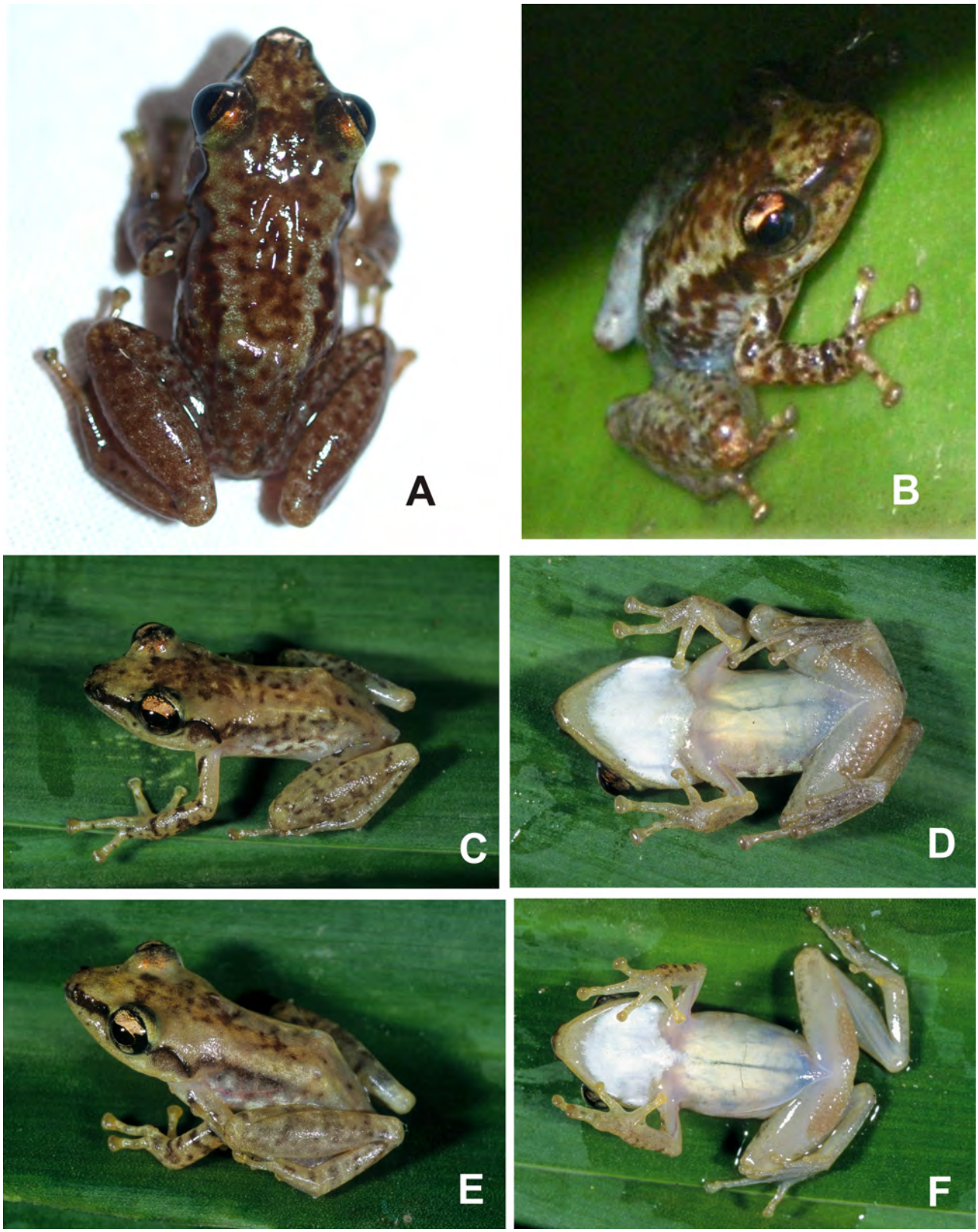

FIGURE 10. Male individuals of *Guibemantis methueni* from Andasibe and Besariaka. (**A–B**) ZSM 3223/2012, (ZCMV 14089) from Andasibe. (**C–D**) ZSM 391/2004 (ZCMV 933) from Besariaka. (**E–F**) Specimen from Besariaka that cannot be reliably assigned to a voucher specimen and is assigned to *G. methueni* based on morphology.

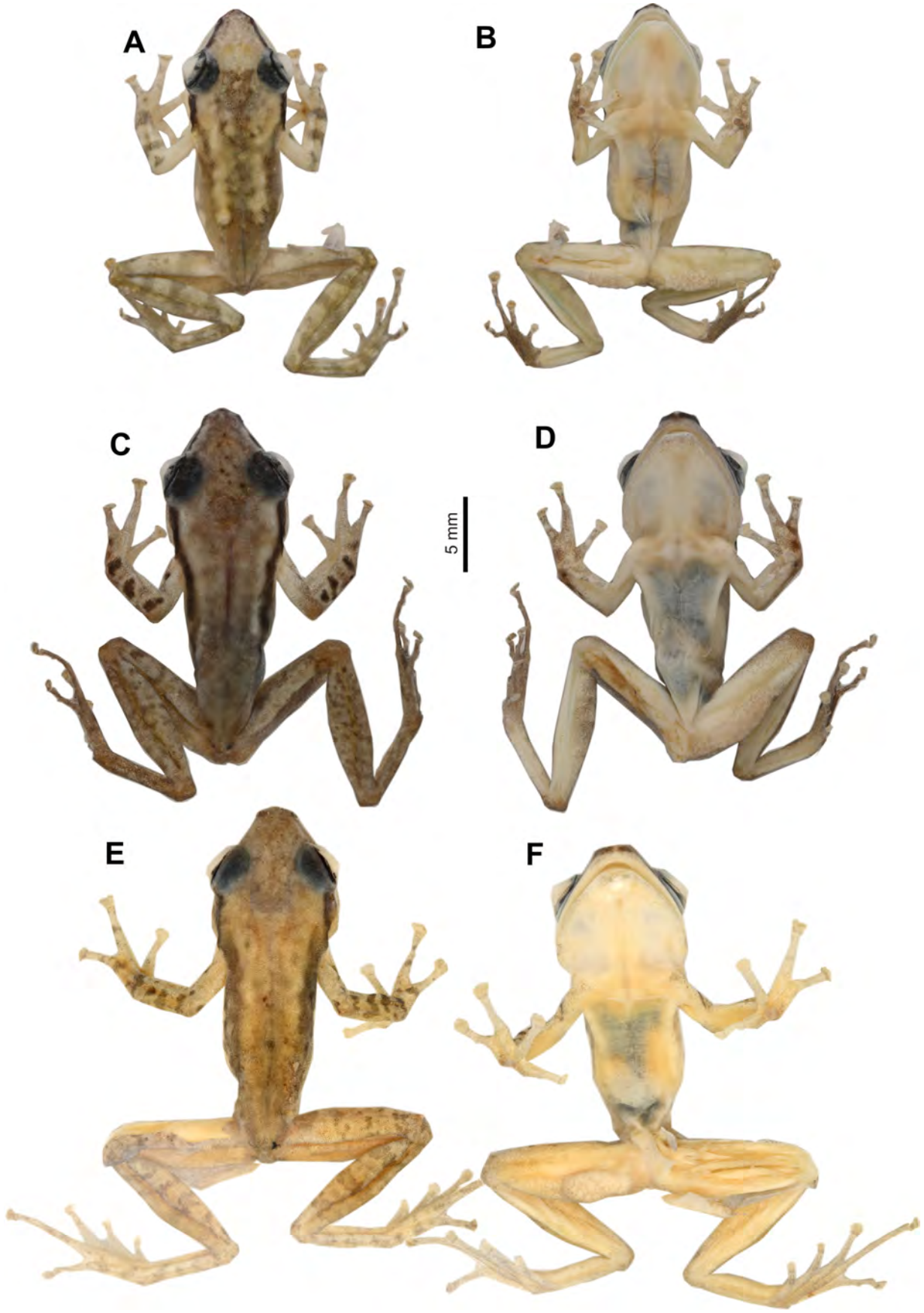

FIGURE 11. Dorsal and ventral views of preserved holotypes of new *Guibemantis* species: **A–B.** *Guibemantis rianasoa* **sp. nov.** (sp. Ca14), male holotype ZSM 149/2022 (ZCMV 13705); **C–D.** *Guibemantis ambakoana* **sp. nov.** (sp. Ca3), male holotype ZSM 152/2022 (ZCMV 13707); **E, F.** *Guibemantis vakoa* **sp. nov.** (sp. Ca8), male holotype ZSM 389/2004 (ZCMV 931).

The new species is characterized by the combination of the following characters: (1) small size with adult SVL up to 24 mm in males (females unknown), (2) light brownish dorsal color, often without distinct darker markings or spots, (3) distinct brown rostral stripe, (4) a few, small whitish spots on (posterior) flanks, (5) absence of distinct dorsolateral stripes, (6) absence of webbing on hand and only traces of web on foot, (7) vomerine teeth present, (8) femoral (macro)glands of males distinct, very clearly recognizable and of contrasting orange-brown color in life, single gland granules well recognizable externally in life and preservative.

Although this combination of character states will allow a distinction from most other species of *Guibemantis*, it is more difficult to diagnose the species against other brownish-colored species, especially *G. ambakoana, G. bicalcaratus, G. methueni,* and *G. wattersoni*. The new species can be reliably diagnosed from all other *Guibemantis* species based on nucleotide positions in the mitochondrial 16S rRNA gene: MolD identified a robust diagnostic nucleotide combination of an 'G' in the site 998, 'A' in the site 1132, 'C' in the site 1251 (positions relative to the full 16S rRNA gene of *Mantella madagascariensis*).

Diagnosis. Distinction from *G. fotsitenda, G. liber, G. razandry, G. razoky* and *G. tasifotsy*: male femoral gland consisting of a well-delimited field of discrete enlarged single gland granules (vs. a diffuse field of small granules covering most of the ventral shank), occurrence limited to *Pandanus* leaf axils (vs. calling and breeding in open swamps), and calls emitted from *Pandanus* vs. calls emitted from exposed perches above swamps.

Distinction from *G. albolineatus*: absence of well-delimited dorsolateral bands (vs. presence), and light brown ground color on dorsum (vs. chocolate-brown).

Distinction from *G. albomaculatus*: absence of fine white dotting on body (vs. presence, especially on hindlimbs and sometimes on dorsum), and males with white color only laterally on throat (vs. white color covering most of the throat).

Distinction from *G. ambakoana*: absence of light dorsolateral bands (vs. presence).

Distinction from *G. annulatus*: absence of a regular pattern of small dark dots dorsally (vs. presence), and absent or poorly contrasted light ring proximal to finger and toe discs (vs. distinct and contrasted).

Distinction from *G. bicalcaratus*: presence of a black vertical line in upper part of iris (vs. absence), and a weakly pigmented grayish flank with a few silvery white markings (vs. flanks of similar color as dorsum and without silvery markings).

Distinction from *G. flavobrunneus*: smaller body size (male SVL 23–24 mm vs. ≥30 mm), and dorsum more or less uniformly brown (vs. brown with contrasted light brown pattern).

Distinction from *G. methueni*: largely uniformly colored dorsum (vs. usually dark markings or spots on dorsum), femoral glands typically with contrasting yellow-orange color (vs. without contrasting color), and males with white color only laterally on throat (vs. white color covering most of throat).

Distinction from *G. milingilingy*: absence of dorsolateral bands (vs. broad and continuous dorsolateral bands), and dorsal color brown typically without greenish shade (vs. yellowish green dorsolateral bands and dorsal markings).

Distinction from *G. pulcher* and *G. pulcherrimus*: brown dorsal color (vs. translucent green), and absence of purple-reddish dots and markings on the dorsum (vs. presence).

Distinction from *G. punctatus*: absence of a regular pattern of small dark dots dorsally (vs. presence).

Distinction from *G. rianasoa*: larger body size (male SVL 23–24 mm vs. ≤20 mm), brown dorsal color (vs. olive greenish), and large femoral glands with contrasting yellowish color in males (vs. small and inconspicuously colored).

Distinction from *G. wattersoni*: absence of dorsolateral bands (vs. poorly contrasted bands usually present), and presence of a black vertical line in upper part of iris (vs. absence).

Distinction from *G. woosteri*: absence of dorsolateral bands (vs. poorly contrasted dorsolateral bands present), and a brown dorsal color without greenish elements (vs. often a green shade, especially of dorsolateral bands).

Description of the holotype. Adult male in good state of preservation (Fig. 11). Tissue removed from ventral side of left thigh for DNA extraction. Head longer than wide and wider than body; snout pointed in dorsal and ventral views, more rounded in lateral view; canthus rostralis straight, loreal region flat; nostrils nearer to tip of snout than to eye, tympanum distinct, 43% of horizontal eye diameter; supratympanic fold distinct, curved; vomerine odontophores distinct, located medially between eye and choanae on either side of head; maxillary teeth present; tongue ovoid, and distinctly bifid at its tip. Arms slightly slender; relative finger length 1<2<4<3, second finger very slightly shorter than fourth finger; finger discs moderately enlarged and squared off at tips in a rounded ‘T’

shape, no webbing between fingers recognizable, subarticular tubercles distinct, unpaired. Hindlimbs moderately slender, foot length 91% of tibia length; lateral metatarsalia largely connected by muscular tissue; inner metatarsal tubercle oblong and recognizable, relatively small; outer metatarsal tubercle round, small and distinct; only traces of webbing recognizable between toes, relative length of toes 1<2<5<3<4, third toe slightly shorter than fifth; toe discs moderately enlarged. Femoral glands distinct and prominent. For morphometric measurements see Table 1.

After almost 20 years in preservative (Fig. 11), dorsal surface is beige with indistinct brownish spots and markings. The flanks are darker brown. No obvious light dorsolateral bands are recognizable. Forelimbs and hindlimbs beige-grayish, with brown crossbands. Ventral side beige. In life (Fig. 9), dorsal surface was golden brown with a few dark brown spots, a dark brown rostral stripe was present, and limbs were grayish brown with dark brown spots and crossbands. A few silvery white spots were visible on the posterior flanks. Ventrally, mostly unpigmented/translucent, with very little white pigment on throat. Femoral glands were very distinct and contrasted, of orange-brown color.

Variation. The known males all have distinct brown-orange femoral glands and only a little amount of white color laterally on the throat (Fig. 9). Females are unknown.

Etymology. The species name is derived from the Malagasy word "vakoa", used in eastern Madagascar to refer to *Pandanus* screw pines and used to highlight the occurrence of this species in *Pandanus* leaf axils. The name is used as a noun in apposition.

Natural history. Very poorly known. Specimens were found on 15 February 2004 in a forest fragment near Besariaka (destroyed by slash-and-burn agriculture two years later) in *Pandanus* plants, calling during the day. At Besariaka, specimens occurred in syntopy with *G. methueni*.

Bioacoustics. Advertisement calls recorded on 15 February 2004 at Besariaka (air temperature 21°C; Fig. 4C) consist of a single very short click-note, emitted at long, somewhat irregular intervals. Amplitude modulation is evident in each call, with maximum call energy present at the beginning of the call, gradually decreasing towards the call's end. Numerical parameters of 28 analysed calls from at least two individuals are as follows: call duration (= note duration) 8–14 ms (10.2 ± 1.7 ms); inter-call intervals 623–1286 ms (869.5 ± 214.3 ms); dominant frequency 3521–3972 Hz (3720 ± 206 Hz); prevalent bandwidth 2000–5500 Hz. Call repetition rate was approximately between 65–85 calls/minute.

Calls recorded in 2007 at Betampona (Rosa *et al.* 2011, track 27, as *G.* sp. aff. *bicalcaratus*) agree in character with those reported from Besariaka in consisting of a single very short click-note emitted at variable, but long intervals. Numerical parameters of 32 analysed calls are as follows: call duration (= note duration) 3–9 ms (5.9 ± 1.9 ms); inter-call intervals 471–1470 ms (767.9 ± 363.8 ms); dominant frequency 3423–3779 Hz (3576 ± 135 Hz); prevalent bandwidth 2000–5700 Hz.

Distribution. Besides (1) the type locality Besariaka, the species has also been recorded, based on genetic evidence, from (2) Sahafina, (3) Betampona, and (4) Fierenana (Figs 1–2).

Discussion

The description of three new species in this study brings the number of *Pandanusicola* up to 21. This is more than three times the number of species in the nominal subgenus *Guibemantis* (currently six species), which might indicate that phytotelmic specialization along with smaller body size (see Wollenberg *et al.* 2011) of *Pandanusicola* may have influenced their diversification. Furthermore, at least one of the new species (*G. rianasoa*) is morphologically distinct in various characters and represents a phylogenetically isolated lineage (Fig. 1), exemplifying that the rise in species diversity is due to true discovery of biologically divergent species rather than "over-splitting" of previously known taxa.

Admittedly, the scarcity of available advertisement call recordings and the overall high intra-lineage variation in coloration, combined with the otherwise conservative external morphology of *Pandanusicola* frogs, pose substantial challenges to convincingly delimit and diagnose species in this subgenus. In a recent taxonomic revision of *Gephyromantis* frogs (Miralles *et al.* 2023), we opted to present the respective support for each species limit among each pairwise combination of lineages in a matrix format, but this format to summarize species limits would be extremely difficult to achieve in a species-rich clade such as *Pandanusicola*. It is important to keep in mind that in the rationale used here, we do not consider morphological differences as mandatory to accept two lineages as species. In this, we agree with other authors (e.g., Jörger & Schrödl 2013; Delić *et al.* 2017; Fišer *et al.* 2018) who

supported describing and formally naming morphologically cryptic species, not the least to facilitate their study in an evolutionary framework and their inclusion in conservation management (Delić *et al.* 2017).

In the case of *Pandanusicola*, the newly described *G. ambakoana* and *G. vakoa* are difficult to distinguish unambiguously by morphology alone from other predominantly brown-colored species of *Pandanusicola*, such as *G. albolineatus, G. albomaculatus, G. annulatus, G. bicalcaratus, G. punctatus, G. wattersoni, G. woosteri*, but for the purpose of species delimitation, many of these species can already be excluded from the comparisons as they belong to other clades according to molecular phylogenetic data (Koppetsch *et al.* 2023). As elaborated in detail in the Species Delimitation section of Results, most important to determining species limits was the observation of several of our focal species occurring in close syntopy (e.g., *G. ambakoana, G. methueni,* and *G. rianasoa* at Andasibe; *G. methueni* and *G. vakoa* at Besariaka) under the maintenance of clear morphological differences and without genetic admixture. Although we are aware that species delimitation in *Pandanusicola* is still plagued by missing data (e.g., lack of multigene data on the phylogenetic position of *G. bicalcaratus;* lack of bioacoustic data for many species, including *G. albolineatus, G. albomaculatus, G. punctatus, G. woosteri*), we are convinced that the taxonomic hypothesis proposed here, distinguishing *G. ambakoana, G. rianasoa* and *G. vakoa* as additional new species, better reflects biological reality and facilitates future research and conservation activities on these frogs.

In fact, our taxonomic hypothesis is highly conservative in many aspects, and we provisionally included several genetically divergent lineages in known taxa (e.g., *G.* cf. *rianasoa* from Fierenana; *G.* cf. *ambakoana* from Maharira in Ranomafana National Park; *G. albolineatus* from Ranomafana; *G. flavobrunneus* from Ranomafana). These individuals represent genetically divergent populations that occur at a substantial geographical distance from their closest relatives according to the 16S tree (Fig. 1), and therefore an argument of sympatric occurrence without genetic admixture at present cannot be invoked to test their possible species distinctness. Nonetheless, these frogs warrant further taxonomic scrutiny in the future. The same is true for multiple candidate species included in our phylogenetic tree (Fig. 1), of which five were newly assigned with provisional candidate species names in this paper, following the numbering scheme of Vieites *et al.* (2009) and Perl *et al.* (2014): *G.* sp. Ca22 to Ca26. Discussing all these lineages in detail is beyond the scope of the present paper, but it is important to emphasize that for most of them, fewer samples and biological data are available compared to the species described herein, and the taxonomic revision of at least some will depend on additional field work. As exemplified by *G. ambakoana*, which apparently includes two highly divergent mitochondrial lineages in Andasibe (lineages A and E), mitochondrial data alone can be misleading in cases of putative hybridization and admixture. As such, we emphasize that a careful integrative analysis (Padial *et al.* 2010) should precede the formal scientific naming of any of these candidate species.

The small size of *G. rianasoa*, with adult males as small as 18 mm SVL and with inconspicuous femoral glands, raises the possibility of even further taxonomic complexity of the subgenus across Madagascar. Individuals from other populations previously identified as subadults (and therefore often not collected/sampled) may warrant additional examination, especially given that small size in mantellids is associated with increased genetic diversity (Pabijan *et al.* 2012). Interestingly, in 2022, *G. rianasoa* was found to be relatively common in the Andasibe area; it remains unknown if there has been an increase in its local distribution and/or population density, or if the previous lack of observation of this species is due to them being overlooked and mistaken for subadults in the past.

The *Pandanus* obligate species of *Guibemantis* in general have relatively quiet calls (Lehtinen *et al.* 2012), and these have been recorded and thoroughly described only for a limited number of species. Because it is challenging to collect individual frogs after observing them calling among the spiny *Pandanus* leaves, some minimal uncertainties remain about the correct assignment of the calls of *G. ambakoana* and *G. rianasoa* (see above). Yet, overall, a picture emerges where sympatric species of *Pandanus* obligate species do differ bioacoustically. For instance, the trill-like call of *G. methueni* that was recorded from multiple geographically distant populations of this species differs from all other *Pandanusicola* calls known to date (somewhat reminding only of *G. tasifotsy*; Lehtinen *et al.* 2012). Another important observation is that the duration (and amplitudal character) of calls differ among the sympatric species around Andasibe, which are relatively static variables not heavily influenced by temperature or body size (Köhler *et al.* 2017), therefore constituting stable differences in bioacoustic signals.

Co-occurrence and niche partitioning have been matters of intense study in the field of ecology, as shown in MacArthur & Levins (1967), Roughgarden (1976), and Vacher *et al.* (2016), to name a few. Lehtinen & Carfagno (2011) observed a 19.8% co-occurrence rate between two *Guibemantis* species in the South East of Madagascar, which was attributed to the niche of a superiorly competitive species completely overlapping that of a competitively inferior species. In the absence of further habitat data (diet, water level in plants, tree species, detritus level, canopy

cover, etc.), and given the 30% rate of co-occurrence observed in April 2022, our data suggest that body size is the biggest difference between the novel *Guibemantis* species. In order to determine if these frogs are demonstrating a classic niche partitioning or an included niche mechanism, further research on their diet, reproduction and larval stages is needed, as well as their relationships with the other species found in *Pandanus*. For example, *Damastes* spiders observed in *Pandanus* during the April 2022 survey could easily prey on the same arthropods as frogs, or even on frogs themselves (Fulgence *et al.* 2020).

Although the co-occurrence of various species of *Pandanus* obligate frogs has been well documented in the past, the area around Andasibe appears to host the largest number of species in sympatry to date. Leaving aside *G. liber*, which uses *Pandanus* axils as shelter but not for reproduction, the area hosts (1) the large-sized *G. flavobrunneus* that, however, was not found in our 2022 surveys and appears to have a rather spotty occurrence; (2) the rather easily diagnosable *G. pulcher,* characterized by translucent-green color and purplish-brown spotting; (3) *G. methueni*, which according to our data is the predominant coastal species in the Northern Central East geographical region but can be found at ca. 900 m a.s.l. near Andasibe, and the three new species described herein, (4) *G. ambakoana*, (5) *G. vakoa*, and (6) *G. rianasoa*. Except for *G. vakoa*, all of these species have been encountered within a few kilometers around the village of Andasibe. As such, Andasibe would be an ideal site to further study their ecological niche partitioning, both in the adult and larval stages, for which the description of three new *Pandanusicola* species herein provides a taxonomic basis. More generally, the taxonomic inventory of the herpetofauna at popular tourist sites like Andasibe is important not only for conservation management but also for maximizing the ecotourism opportunities of Madagascar's unique herpetofauna (Wollenberg *et al.* 2011).

Acknowledgments

We acknowledge the help and assistance received from numerous colleagues, students, and guides during a large number of field expeditions in Madagascar, in particular Rainer Dolch, Alida Hasiniaina, Evariste Desire, Christin Nasoavina, Eleni Bethke, Fanomezana M. Ratsoavina, and Solohery Rasamison. Special thanks go to Philip-Sebastian Gehring who collected many samples along Madagascar's east coast that were included in this study. The research was carried out in the framework of collaboration accords between the Zoological Institute of TU Braunschweig, the Zoologische Staatssammlung München, the Mention Zoologie et Biodiversité Animale of the Université d'Antananarivo, and the Ministère de l'Environnement, des Eaux et des Forêts of the Republic of Madagascar. We are grateful to the Malagasy authorities and to Madagascar National Parks for research, and export permits (research permits 21/22/22/MEDD/SG/DGGE/DAPRNA/SCBE.Re issued 8 February 2022 and 297/22/MEDD/SG/DGGE/DAPRNA/SCBE.Re issued 13 October 2022; export permit 199N-EA05/MG23 issued 23 May 2023).

References

AmphibiaWeb (2023) Information on amphibian biology and conservation. AmphibiaWeb, Berkeley, California. Available from: http://amphibiaweb.org/ (accessed 26 July 2023)

Avise, J.C. & Ball, R.M. (1990) Principles of genealogical concordance in species concepts and biological taxonomy. *In*: Futuyma, D. & Antonovics, J. (Eds.), *Oxford Surveys in Evolutionary Biology*. Oxford University Press, Oxford, pp. 45–67.

Bletz, M.C., Scherz, M.D., Rakotoarison, A., Lehtinen, R.M., Glaw, F. & Vences, M. (2018) Stumbling upon a new frog species of *Guibemantis* (Anura: Mantellidae) on the top of the Marojejy massif in northern Madagascar. *Copeia*, 106, 255–263. https://doi.org/10.1643/CH-17-655

Blommers-Schlösser, R.M.A. (1975) A unique case of mating behaviour in a Malagasy tree frog, *Gephyromantis liber* (Peracca 1893), with observations on the larval development (Amphibia, Ranidae). *Beaufortia*, 23, 15–23.

Blommers-Schlösser, R.M.A. (1979) Biosystematics of the Malagasy frogs. I. Mantellinae (Ranidae). *Beaufortia*, 29, 1–77.

Boumans, L., Vieites, D.R., Glaw, F. & Vences, M. (2007) Geographical patterns of deep mitochondrial differentiation in widespread Malagasy reptiles. *Molecular Phylogenetics and Evolution*, 45, 822–839. https://doi.org/10.1016/j.ympev.2007.05.028

Brown, J.L., Cameron, A., Yoder, A.D. & Vences, M. (2014) A necessarily complex model to explain the biogeography of the amphibians and reptiles of Madagascar. *Nature Communications*, 5, e5046. https://doi.org/10.1038/ncomms6046

Brown, J.L., Sillero, N., Glaw, F., Bora, P., Vieites, D.R. & Vences, M. (2016) Spatial biodiversity patterns of Madagascar's

amphibians and reptiles. *PloS ONE*, 11, e0144076.
https://doi.org/10.1371/journal.pone.0144076
Bruford, M.W., Hanotte, O., Brookfield, J.F.Y. & Burke, T. (1992) Single-locus and multilocus DNA fingerprint. *In*: Hoelzel, A.R. (Ed.), *Molecular Genetic Analysis of Populations: A Practical Approach*. IRL Press, Oxford, pp. 225–270.
Callmander, M.W., Laivao, M.O. & Buerki, S. (2022) Pandanaceae, screw-pines, vakoa, hofa, frandra. *In*: Goodman, S.M. (Ed.), *The New Natural History of Madagascar*. Princeton University Press, Princeton, pp. 551–559.
https://doi.org/10.2307/j.ctv2ks6tbb.67
Chan, K.O., Hertwig, S.T., Neokleous, D.N., Flury, J.M. & Brown, R.M. (2022) Widely used, short 16S rRNA mitochondrial gene fragments yield poor and erratic results in phylogenetic estimation and species delimitation of amphibians. *BMC Ecology and Evolution*, 22, 37.
https://doi.org/10.1186/s12862-022-01994-y.
Colwell, R.K. & Lees, D.C. (2000) The mid-domain effect: geometric constraints on the geography of species richness. *Trends in Ecology & Evolution*, 15, 70–76.
https://doi.org/10.1016/S0169-5347(99)01767-X
Crottini, A., Madsen, O., Poux, C., Strauß, A., Vieites, D.R. & Vences, M. (2012) Vertebrate time-tree elucidates the biogeographic pattern of a major biotic change around the K–T boundary in Madagascar. *Proceedings of the National Academy of Sciences*, 109, 5358–5363.
https://doi.org/10.1073/pnas.1112487109
Delić, T., Trontelj, P., Rendoš, M. & Fišer, C. (2017) The importance of naming cryptic species and the conservation of endemic subterranean amphipods. *Scientific Reports*, 7, 3391.
https://doi.org/10.1038/s41598-017-02938-z
de Queiroz, K. (1998) The general lineage concept of species, species criteria, and the process of speciation. *In*: Howard, D.J. & Berlocher, S.H. (Eds.), *Endless Forms. Species and Speciation*. Oxford University Press, Oxford, pp. 49–89.
de Queiroz, K. (2007) Species concepts and species delimitation. *Systematic Biology*, 56, 879–886.
https://doi.org/10.1080/10635150701701083
Dufresnes, C., Brelsford, A., Jeffries, D.L., Mazepa, G., Suchan, T., Canestrelli, D., Nicieza, A., Fumagalli, L., Dubey, S., Martínez-Solano, I., Litvinchuk, S.N., Vences, M., Perrin, N. & Crochet, P.A. (2021) Mass of genes rather than master genes underlie the genomic architecture of amphibian speciation. *Proceedings of the National Academy of Sciences of the USA*, 118, e2103963118.
https://doi.org/10.1073/pnas.2103963118
Edler, D., Klein, J., Antonelli, A. & Silvestro, D. (2021) raxmlGUI 2.0: a graphical interface and toolkit for phylogenetic analyses using RAxML. *Methods in Ecology and Evolution*, 12, 373–377.
https://doi.org/10.1111/2041-210X.13512
Fedosov, A., Achaz, G., Gontchar, A. & Puillandre, N. (2022) mold, a novel software to compile accurate and reliable DNA diagnoses for taxonomic descriptions. *Molecular Ecology Resources*, 22, 2038–2053.
https://doi.org/10.1111/1755-0998.13590.
Fišer, C., Robinson, C.T. & Malard, F. (2018) Cryptic species as a window into the paradigm shift of the species concept. *Molecular Ecology*, 27, 613–635.
https://doi.org/10.1111/mec.14486
Fouquet, A., Gilles, A., Vences, M., Marty, C., Blanc, M. & Gemmell, N.J. (2007) Underestimation of species richness in Neotropical frogs revealed by mtDNA analyses. *PLoS ONE*, 2, e1109.
https://doi.org/10.1371/journal.pone.0001109
Fulgence, T.R., Martin, D.A., Kreft, H., Ratsoavina, F.M. & Andrianarimisa, A. (2020) Spider traps amphibian in northeastern Madagascar. *Ecology and Evolution*, 11, 682–687.
https://doi.org/10.1002/ece3.7102
Glaw, F., Köhler, J., Crottini, A., Gehring, P.-S., Prötzel, D., Randriamanana, L., Andreone, F. & Vences, M. (2021) An additional level of cryptic diversity: A new green-coloured Malagasy treefrog of the *Boophis luteus* species group. *Salamandra*, 57, 295–308.
Glaw, F. & Vences, M. (1994) *A Fieldguide to the Amphibians and Reptiles of Madagascar. 2nd Edition, including Mammals and Freshwater Fish*. Vences and Glaw Verlag, Cologne.
Glaw, F. & Vences, M. (2006) Phylogeny and genus-level classification of mantellid frogs. *Organisms Diversity and Evolution*, 6, 236–253.
https://doi.org/10.1016/j.ode.2005.12.001
Glaw, F. & Vences, M. (2007) *A Field Guide to the Amphibians and Reptiles of Madagascar, 3rd Edition*. Vences and Glaw Verlag, Cologne, 496 pp.
Glaw, F., Vences, M. & Gossmann, V. (2000) A new species of *Mantidactylus* (subgenus *Guibemantis)* from Madagascar, with a comparative survey of internal femoral gland structure in the genus (Amphibia: Ranidae: Mantellinae). *Journal of Natural History*, 34, 1135–1154.
https://doi.org/10.1080/00222930050020140
Goodman, S.M. (2010) Biological research conducted in the general Andasibe region of Madagascar with emphasis on enumerating the local biotic diversity. *Malagasy Nature*, 3, 13–34.

Guillaumet, J.L. (1973) Formes et développement des «*Pandanus*» malgaches. *Webbia*, 28 (2), 495–519. https://doi.org/10.1080/00837792.1973.10670009
Heinermann, J., Rodríguez, A., Segev, O., Edmonds, D., Dolch, R. & Vences, M. (2015) Year-round activity patterns in a hyperdiverse community of rainforest amphibians in Madagascar. *Journal of Natural History*, 49, 2213–2231. https://doi.org/10.1080/00222933.2015.1009513
Jörger, K.M. & Schrödl, M. (2013) How to describe a cryptic species? Practical challenges of molecular taxonomy. *Frontiers in Zoology*, 10, 59. https://doi.org/10.1186/1742-9994-10-59
Katoh, K. & Standley, D.M. (2013) MAFFT multiple sequence alignment software version 7: improvements in performance and usability. *Molecular Biology and Evolution*, 30, 772–780. https://doi.org/10.1093/molbev/mst010
Köhler, J., Jansen, M., Rodríguez, A., Kok, P.J.R., Toledo, L.F., Emmrich, M., Glaw, F., Haddad, C.F.B., Rödel, M.O. & Vences, M. (2017) The use of bioacoustics in anuran taxonomy: theory, terminology, methods and recommendations for best practice. *Zootaxa*, 4251 (1), 1–124. https://doi.org/10.11646/zootaxa.4251.1.1
Koppetsch, T., Pabijan, M., Hutter, C.R., Köhler, J., Gehring, P.-S., Rakotoarison, A., Ratsoavina, F.M., Scherz, M.D., Vieites, D.R., Glaw, F. & Vences, M. (2023) An initial molecular resolution of the mantellid frogs of the *Guibemantis liber* complex reveals three new species from northern Madagascar. *Vertebrate Zoology*, 73, 397–432. https://doi.org/10.3897/vz.73.e94063
Kumar, S., Stecher, G. & Tamura, K. (2016) MEGA7: Molecular Evolutionary Genetics Analysis version 7.0 for bigger datasets. *Molecular Biology and Evolution*, 33, 1870–1874. https://doi.org/10.1093/molbev/msw054
Lees, D.C. (1994) The Périnet effect? Diversity gradients in an adaptive radiation of butterflies in Madagascar (Satyrinae: Mycalesina) compared with other rainforest taxa. *In:* Lourenço W.R. (Ed.), *Biogéographie de Madagascar*. Editions de l'ORSTOM 1996, Paris, pp. 479–90.
Lehtinen, R.M. (2002) The use of screw pines (*Pandanus* spp.) by amphibians and reptiles in Madagascar. *Herpetological Bulletin*, 82, 20–25.
Lehtinen, R.M. (2003) Parental care and reproduction in two species of *Mantidactylus* (Anura: Mantellidae). *Journal of Herpetology*, 37, 766–768. https://doi.org/10.1670/87-03N
Lehtinen, R.M. (2004) Tests for competition, cannibalism, and priority effects in two phytotelm-dwelling tadpoles from Madagascar. *Herpetologica*, 60, 1–13. https://doi.org/10.1655/02-88
Lehtinen, R.M. (2005) Competitive interactions and distributional dynamics in two Malagasy frogs. *Journal of Tropical Ecology*, 21, 569–576. https://doi.org/10.1017/S0266467405002580
Lehtinen, R.M. (2009) The natural history of two plant-breeding frogs from Madagascar, *Guibemantis bicalcaratus* and *G. punctatus* (Anura: Mantellidae). *Salamandra*, 45, 39–49.
Lehtinen, R.M., Glaw, F., Andreone, F., Pabijan, M. & Vences, M. (2012) A new species of putatively pond breeding frog of the genus *Guibemantis* from Madagascar. *Copeia*, 2012, 648–662. https://doi.org/10.1643/CH-11-128
Lehtinen, R.M., Glaw, F., Vences, M., Rakotoarison, A. & Scherz, M.D. (2018) Two new *Pandanus* frogs (*Guibemantis*: Mantellidae: Anura) from northern Madagascar. *European Journal of Taxonomy*, 451, 1–20. https://doi.org/10.5852/ejt.2018.451
Lehtinen, R.M., Glaw, F. & Vences, M. (2011) Two new plant-breeding frog species (Anura: Mantellidae, *Guibemantis*) from southeastern Madagascar. *Herpetological Journal*, 21, 95–112.
Lehtinen, R.M. & Carfagno, G.L. (2011) Habitat selection, the included niche, and coexistence in plant-specialist frogs from Madagascar. *Biotropica*, 43, 58–67. https://doi.org/10.1111/j.1744-7429.2010.00730.x
Lehtinen, R.M., Nussbaum, R.A., Richards, C.M., Cannatella, D.C. & Vences, M. (2007) Mitochondrial genes reveal cryptic diversity in plant-breeding frogs from Madagascar (Anura, Mantellidae, *Guibemantis*). *Molecular Phylogenetics and Evolution*, 44, 1121–1129. https://doi.org/10.1016/j.ympev.2007.05.020
Librado, P. & Rozas, J. (2009) DnaSP. Version 5. A software for comprehensive analysis of DNA polymorphism data. *Bioinformatics*, 25, 1451–1452. https://doi.org/10.1093/bioinformatics/btp187
MacArthur, R. & Levins, R. (1967) The limiting similarity, convergence, and divergence of coexisting species. *The American Naturalist*, 101, 377–385. https://doi.org/10.1086/282505
Miralles, A., Köhler, J., Glaw, F., Wollenberg Valero, K.C., Crottini, A., Rosa, G.M., du Preez, L., Vieites, D.R., Ratsoavina, F.M. & Vences, M. (2023) An endless harvest: integrative revision of the *Gephyromantis boulengeri* and *G. blanci* complexes

reveals six new species of mantellid frogs from Madagascar. *Salamandra*, 59, 1–41.
Moat, J. & Smith, P. (2007) *Atlas of the Vegetation of Madagascar*. Royal Botanic Gardens, Kew, 124 pp.
Pabijan, M., Wollenberg, K.C. & Vences, M. (2012) Small body size increases the regional differentiation of populations of tropical mantellid frogs (Anura: Mantellidae). *Journal of Evolutionary Biology*, 25, 2310–2324. https://doi.org/10.1111/j.1420-9101.2012.02613.x
Padial, J.M., Miralles, A., De la Riva, I. & Vences, M. (2010) The integrative future of taxonomy. *Frontiers in Zoology*, 7, 16. https://doi.org/10.1186/1742-9994-7-16
Palumbi, S.R., Martin, A., Romano, S., McMillan, W.O., Stice, L. & Grabowski, G. (1991) *The Simple Fool's Guide to PCR, Version 2.0*. Privately published, University of Hawaii, Honolulu.
Perl, R.G.B., Nagy, Z.T., Sonet, G., Glaw, F., Wollenberg, K.C. & Vences, M. (2014) DNA barcoding Madagascar's amphibian fauna. *Amphibia-Reptilia*, 35, 197–206. https://doi.org/10.1163/15685381-00002942
Puillandre, N., Brouillet, S. & Achaz, G. (2021) ASAP: Assemble Species by Automatic Partitioning. *Molecular Ecology Resources*, 21, 609–620. https://doi.org/10.1111/1755-0998.13281
Pyron, R.A., O'Connell, K.A., Duncan, S.C., Burbrink, F.T. & Beamer, D.A. (2023) Speciation hypotheses from phylogeographic delimitation yield an integrative taxonomy for seal salamanders (*Desmognathus monticola*). *Systematic Biology*, 72, 179–197. https://doi.org/10.1093/sysbio/syac065
Rosa, G.M., Márquez, R. & Andreone, F. (2011) *The astonishing calls of the frogs of Betampona*. Museo Regionale di Scienze Naturali di Torino & Fonoteca Madrid, Torino. [CD and booklet]
Roughgarden, J. (1976) Resource partitioning among competing species—a coevolutionary approach. *Theoretical Population Biology*, 9, 388–424. https://doi.org/10.1016/0040-5809(76)90054-X
Salzburger, W., Ewing, G.B. & Von Haeseler, A. (2011) The performance of phylogenetic algorithms in estimating haplotype genealogies with migration. *Molecular Ecology*, 20, 1952–1963. https://doi.org/10.1111/j.1365-294X.2011.05066.x
Scherz, M.D., Crottini, A., Hutter, C.R., Hildenbrand, A., Andreone, F., Fulgence, T.R., Köhler, G., Ndriantsoa, S.H., Ohler, A., Preick, M., Rakotoarison, A., Rancilhac, L., Raselimanana, A.P., Riemann, J.C., Rödel, M.-O., Rosa, G.M., Streicher, J.W., Vieites, D.R., Köhler, J., Hofreiter, M., Glaw, F. & Vences, M. (2022) An inordinate fondness for inconspicuous brown frogs: integration of phylogenomics, archival DNA analysis, morphology, and bioacoustics yields 24 new taxa in the subgenus *Brygoomantis* (genus *Mantidactylus*) from Madagascar. *Megataxa*, 7 (2), 113–311. https://doi.10.11646/megataxa.7.2.1
Scherz, M.D., Glaw, F., Hutter, C.R., Bletz, M.C., Rakotoarison, A., Köhler, J. & Vences, M. (2019) Species complexes and the importance of Data Deficient classification in Red List assessments: The case of *Hylobatrachus* frogs. *PLoS One*, 14, e0219437. https://doi.org/10.1371/journal.pone.0219437
Shen, X.X., Liang, D. & Zhang, P. (2012) The development of three long universal nuclear protein-coding locus markers and their application to osteichthyan phylogenetics with nested PCR. *PLoS One*, 7, e39256. https://doi.org/10.1371/journal.pone.0039256
Speybroeck, J., Beukema, W., Dufresnes, C., Fritz, U., Jablonski, D., Lymberakis, P., Martínez-Solano, I., Razzetti, E., Vamberger, M., Vences, M., Vörös, J. & Crochet, P. (2020) Species list of the European herpetofauna – 2020 update by the Taxonomic Committee of the Societas Europaea Herpetologica. *Amphibia-Reptilia*, 41, 139–189. https://doi.org/10.1163/15685381-bja10010
Stamatakis, A. (2014) RAxML version 8: A tool for phylogenetic analysis and post-analysis of large phylogenies. *Bioinformatics*, 30, 1312–1313. https://doi.org/10.1093/bioinformatics/btu033
Stephens, M., Smith, N.J. & Donnelly, P. (2001) A new statistical method for haplotype reconstruction from population data. *American Journal of Human Genetics*, 68, 978–989. https://doi.org/10.1086/319501
Vacher, C., Tamaddoni-Nezhad, A., Kamenova, S., Peyrard, N., Moalic, Y., Sabbadin, R., Schwaller, L., Chiquet, J., Smith, M.A., Vallance, J., Fievet, V., Jakuschkin, B. & Bohan, D.A. (2016) Learning ecological networks from next-generation sequencing data. *Advances in Ecological Research*, 54, 1–39. https://doi.org/10.1016/bs.aecr.2015.10.004
Vences, M., Glaw, F. & Marquez, R. (2006) *The Calls of the Frogs of Madagascar. 3 Audio CD's and booklet*. Alosa, Barcelona, 44 pp.
Vences, M., Hauswaldt, S. & Glaw, F. (2011) The advertisement call of *Guibemantis pulcher*, a phytotelmic frog from Madagascar. *Herpetology Notes*, 4, 377–379
Vences, M., Hutter, C., Glaw, F., Rakotoarison, A., Raselimanana, A. & Scherz, M. (2023) A new species of *Pandanus*-dwelling frog from northern Madagascar related to *Guibemantis pulcher*. *Zootaxa*, 5306 (1), 97–115. https://doi.org/10.11646/zootaxa.5306.1.4

Vences, M., Köhler, J., Andreone, F., Craul, A.-K., Crottini, A., du Preez, L., Preick, M., Rancilhac, L., Rödel, M.-O., Scherz, M.D., Streicher, J.W., Hofreiter, M. & Glaw, F. (2021a): Target-enriched DNA sequencing clarifies the identity of name-bearing types of the *Gephyromantis plicifer* complex and reveals a new species of mantellid frog from Madagascar. *Spixiana*, 44, 175–202.

Vences, M., Miralles, A., Brouillet, S., Ducasse, J., Fedosov, A., Kharchev, V., Kostadinov, I., Kumari, S., Patmanidis, S., Scherz, M.D., Puillandre, N. & Renner, S.S. (2021b) iTaxoTools 0.1: Kickstarting a specimen-based software toolkit for taxonomists. *Megataxa*, 6 (2), 77–92.
https://doi.org/10.11646/megataxa.6.2.1

Vences, M., Patmanidis, S., Kharchev, V. & Renner, S.S. (2022) Concatenator, a user-friendly program to concatenate DNA sequences, implementing graphical user interfaces for MAFFT and FastTree. *Bioinformatics Advances*, 2, vbac050.
https://doi.org/10.1093/bioadv/vbac050

Vences, M., Rakotoarison, A., Rakotondrazafy, A.M.A., Ratsoavina, F.M., Randrianiaina, R.D., Glaw, F., Lehtinen, R.M. & Raxworthy, C.J. (2013) Assessing the diversity of phytotelmic frogs along Madagascar's east coast: Redefinition of *Guibemantis bicalcaratus* (Boettger, 1913) and revalidation of *Guibemantis methueni* (Angel, 1929). *Vertebrate Zoology*, 63, 193–205.
https://doi.org/10.3897/vz.63.e31427

Vences, M., Wahl-Boos, G., Hoegg, S., Glaw, F., Spinelli Oliveira, E., Meyer, A. & Perry, S. (2007) Molecular systematics of mantelline frogs from Madagascar and the evolution of their femoral glands. *Biological Journal of the Linnean Society*, 92, 529–539.
https://doi.org/10.1111/j.1095-8312.2007.00859.x

Vieilledent, G., Grinand, C., Rakotomalala, F.A., Ranaivosoa, R., Rakotoarijaona, J-R., Thomas Allnutt, T.F. & Achard, F. (2018) Combining global tree cover loss data with historical national forest cover maps to look at six decades of deforestation and forest fragmentation in Madagascar. *Biological Conservation*, 222, 189–197.
https://doi.org/10.1016/j.biocon.2018.04.008.

Vieites, D.R., Wollenberg, K.C., Andreone, F., Köhler, J., Glaw, F. & Vences, M. (2009) Vast underestimation of Madagascar's biodiversity evidenced by an integrative amphibian inventory. *Proceedings of the National Academy of Science of the USA*, 106, 8267–8272.
https://doi.org/10.1073/pnas.0810821106

Wollenberg, K.C., Jenkins, R.K.B., Randrianavelona, R., Rampilamanana, R., Ralisata, M., Ramanandraibe, A., Ramilijaona Ravoahangimalala, O. & Vences, M. (2011) On the shoulders of lemurs: pinpointing the ecotouristic potential of Madagascar's unique herpetofauna. *Journal of Ecotourism*, 10, 101–117.
https://doi.org/10.1080/14724049.2010.511229

Appendix 1: Call description of *Guibemantis methueni*

Advertisement calls recorded on 8 November 2011 at Andasibe (air temperature not measured) consist of a single very short click-note, emitted at rather regular intervals in defined series containing 4–7 calls. Within call series, both, amplitude and frequency modulation is evident, with the initial call of each series exhibiting the lowest call energy and lowest dominant frequency of all calls, whereas subsequent calls show an increase in dominant frequency and increased amplitude. Numerical parameters of 40 analysed calls from two individuals are as follows: call duration (= note duration) 8–19 ms (16.0 ± 3.9 ms); inter-call interval within regular series 75–121 ms (90.6 ± 14.7 ms); number of calls per call series 4–7 (5.0 ± 1.0); duration of call series 377–664 ms (486.1 ± 105.7 ms); dominant frequency 2928–4102 Hz (3677 ± 378 Hz); prevalent bandwidth 2500–7600 Hz. Call rate within series ranged approximately around 540 calls/minute.

Recordings obtained by R. Blommers-Schlösser in the 1970s at Ambila-Lemaitso (Blommers-Schlösser 1979) and re-analyzed herein, are in general agreement with the calls from Andasibe and clearly allocatable to *G. methueni*. Numerical call parameters of 35 analyzed calls are as follows: call duration (= note duration) 12–17 ms (14.6 ± 1.8 ms); inter-call interval within regular series 56–69 ms (60.8 ± 4.1 ms); number of calls per call series 3–6 (5.0 ± 1.2); duration of call series 161–415 ms (320.7 ± 94.2 ms); dominant frequency 4081–4360 Hz (4219 ± 95 Hz); prevalent bandwidth 2500–6500 Hz.

Recordings obtained on 21 November 2022 at Ankanin'ny Nofy are of poor quality (distantly calling individuals and severe background noise) and therefore it is impossible to analyse these in detail. However, by listening to the recording it is possible to recognize short call series being composed of 5–6 calls (apparently with the first call of the series being slightly longer in duration), which likely correspond to *G. methueni*.